Article

Cell Host & Microbe

# Cutaneous Leishmaniasis Induces a Transmissible Dysbiotic Skin Microbiota that Promotes Skin Inflammation

## Graphical Abstract

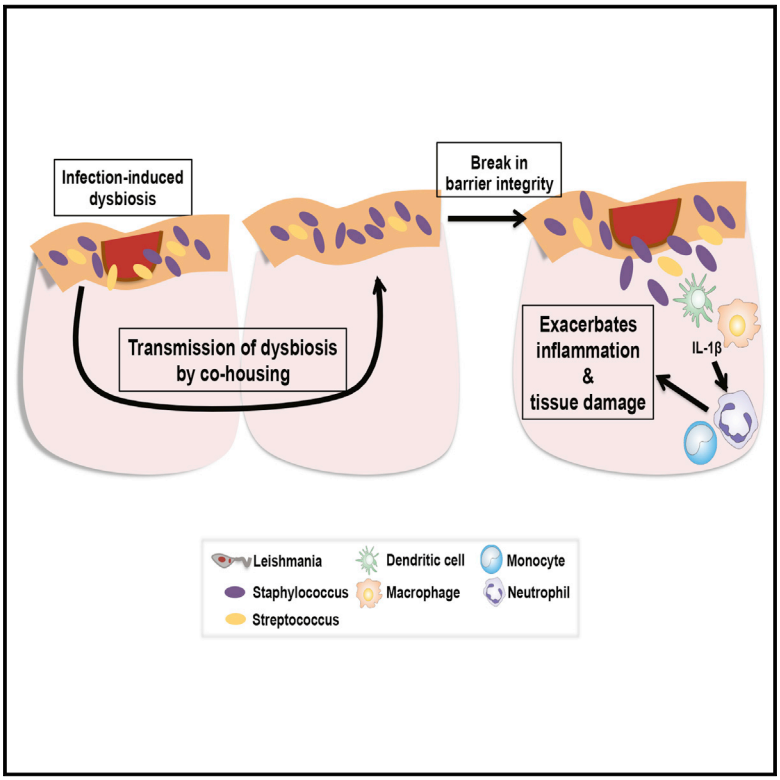


## Authors

Ciara Gimblet, Jacquelyn S. Meisel, Michael A. Loesche, ..., Edgar M. Carvalho, Phillip Scott, Elizabeth A. Grice

## Correspondence

pscott@upenn.edu (P.S.), egrice@upenn.edu (E.A.G.)

## In Brief

The role of skin commensal microbes in dermal cellular responses is largely unknown. Gimblet et al. investigate the role of the skin microbiota during cutaneous leishmaniasis. Leishmania infection creates a dysbiotic skin microbiota that is transmissible to naive skin. Additionally, dysbiosis prior to infection or injury exacerbates skin inflammation.

## Highlights

- Leishmania infection alters the skin microbiota of both humans and mice
- Dysbiosis is characterized by a dominance of *Staphylococcus* and/or *Streptococcus*
- Naive mice acquire dysbiosis when co-housed with leishmania-infected mice
- Acquiring a dysbiotic microbiota prior to infection exacerbates skin inflammation

Gimblet et al., 2017, Cell Host & Microbe *22*, 13–24
July 12, 2017 
http://dx.doi.org/10.1016/j.chom.2017.06.006

Cell Host & Microbe
Article

# Cutaneous Leishmaniasis Induces a Transmissible Dysbiotic Skin Microbiota that Promotes Skin Inflammation

Ciara Gimblet,[1] Jacquelyn S. Meisel,[2] Michael A. Loesche,[2] Stephen D. Cole,[1] Joseph Horwinski,[2] Fernanda O. Novais,[1] Ana M. Misic,[1] Charles W. Bradley,[1] Daniel P. Beiting,[1] Shelley C. Rankin,[1] Lucas P. Carvalho,[4,5,6] Edgar M. Carvalho,[4,5,6] Phillip Scott,[1,*] and Elizabeth A. Grice[2,3,7,*]

[1]Department of Pathobiology, School of Veterinary Medicine, University of Pennsylvania, Philadelphia, PA 19104, USA
[2]Department of Dermatology
[3]Department of Microbiology
Perelman School of Medicine, University of Pennsylvania, Philadelphia, PA 19104, USA
[4]Centro de Pesquisas Gonçalo Moniz, Fundação Oswaldo Cruz, Salvador 40296-710, Brazil
[5]Serviço de Imunologia, Complexo Hospitalar Prof. Edgard Santos, Universidade Federal da Bahia, Salvador 40170-115, Brazil
[6]Instituto Nacional de Ciências e Tecnologia-Doenças Tropicais, Salvador 40110-160, Brazil
[7]Lead Contact
*Correspondence: pscott@upenn.edu (P.S.), egrice@upenn.edu (E.A.G.)
http://dx.doi.org/10.1016/j.chom.2017.06.006

## SUMMARY

**Skin microbiota can impact allergic and autoimmune responses, wound healing, and anti-microbial defense. We investigated the role of skin microbiota in cutaneous leishmaniasis and found that human patients infected with *Leishmania braziliensis* develop dysbiotic skin microbiota, characterized by increases in the abundance of *Staphylococcus* and/or *Streptococcus*. Mice infected with *L. major* exhibit similar changes depending upon disease severity. Importantly, this dysbiosis is not limited to the lesion site, but is transmissible to normal skin distant from the infection site and to skin from co-housed naive mice. This observation allowed us to test whether a pre-existing dysbiotic skin microbiota influences disease, and we found that challenging dysbiotic naive mice with *L. major* or testing for contact hypersensitivity results in exacerbated skin inflammatory responses. These findings demonstrate that a dysbiotic skin microbiota is not only a consequence of tissue stress, but also enhances inflammation, which has implications for many inflammatory cutaneous diseases.**

## INTRODUCTION

The skin is a barrier and the body's first line of defense against injury and infection. It also hosts commensal populations of bacteria, fungi, and viruses that may influence wound healing, the immune response to infection, and inflammatory responses that occur in chronic diseases (Canesso et al., 2014; Grice et al., 2010; Naik et al., 2012). Though there are strong associations between certain human diseases and changes in the skin microbiota (Kong et al., 2012; Loesche et al., 2017; Oh et al., 2013), the consequences of such changes are unclear, including the role of skin commensal microbes in modulating dermal cellular responses. Animal models in which microbial communities can be manipulated are essential to determine whether these changes influence the outcome of disease.

Cutaneous leishmaniasis is caused by intracellular protozoan parasites and is characterized by a spectrum of clinical manifestations, ranging from self-healing single lesions to chronic, and in some cases metastatic, lesions (Scott and Novais, 2016). The factors responsible for chronic disease in leishmaniasis are still being defined, although it is clear that some of the most severe forms of the disease are not caused by uncontrolled parasite replication, but rather an exaggerated immune response leading to excessive inflammation (Antonelli et al., 2005; Lopez Kostka et al., 2009; Santos et al., 2013; Gonzalez-Lombana et al., 2013; Novais et al., 2013; Crosby et al., 2014). Unfortunately, there is no vaccine for leishmaniasis and drug treatment is often ineffective, which provides the impetus for better understanding the factors that drive the destructive inflammatory responses. Some of these severe forms of disease can be mimicked in mice, which can develop healing or non-healing disease following *L. major* infection depending upon whether a dominant Th1 or Th2 response develops (Scott and Novais, 2016). Less well understood is the role the skin microbiota plays in cutaneous leishmaniasis. Although it has been reported that the course of infection in germ-free mice differs from conventional mice (de Oliveira et al., 1999; Naik et al., 2012; Oliveira et al., 2005), how the skin microbiota changes in patients and conventional mice, and whether such changes influence disease, is less clear.

In this study, we found that infection with leishmania parasites causes a decrease in bacterial diversity in the skin that is characterized by communities dominated by *Staphylococcus* spp. and/or *Streptococcus* spp in both humans and mice. We hypothesized that disease-associated shifts in the skin microbiota ("dysbiosis") contribute to lesion pathology and dermal cellular responses, including immune and inflammatory responses in

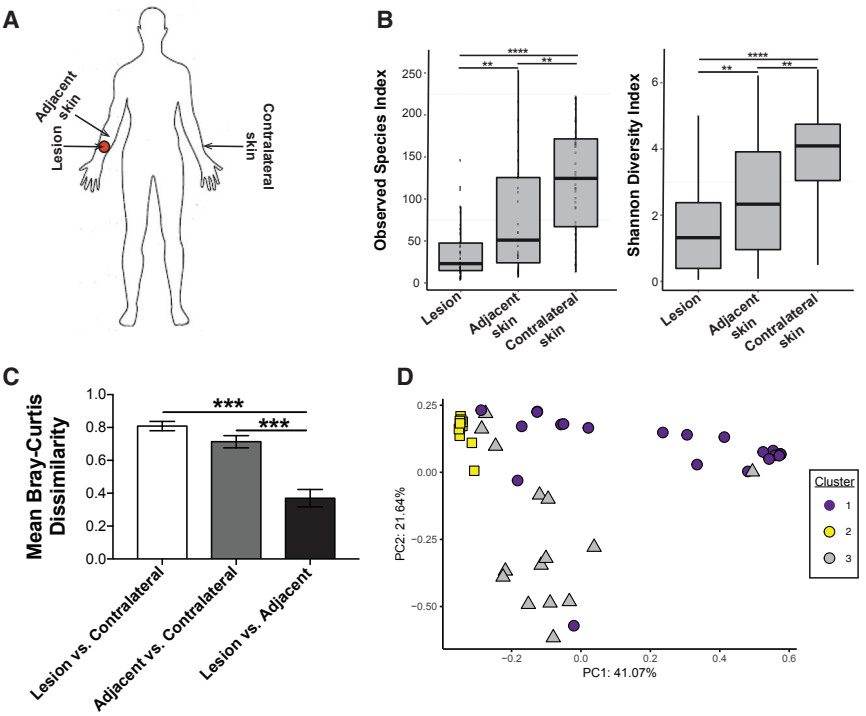


**Figure 1. Lesions from Cutaneous Leishmaniasis Patients Also Have a Dysbiotic Skin Microbiota**

(A) Swabs were collected from the lesion, nearby adjacent skin, and contralateral skin sites for 16S rRNA analysis.

(B) Bacterial diversity was assessed by the number of observed species-level OTUs and Shannon index. Upper and lower box hinges correspond to first and third quartiles, and the distance between these quartiles is defined as the interquartile range (IQR). Lines within the box depict median, and whiskers extend to the highest and lowest values within 1.5 times the IQR. Outliers of the IQR are depicted as dots above or below the whiskers.

(C) Bar charts represent intragroup mean Bray-Curtis dissimilarity between each skin site. Data are presented as mean ± SEM.

(D) PCoA values for weighted UniFrac analysis were plotted and colored based on the Dirichlet multinomial cluster assignment.

(E) Stacked bar charts represent the proportion of the top ten taxa present in each Dirichlet cluster. Swabs were collected from n = 44 patients. $^{**}p < 0.01$; $^{***}p < 0.001$; $^{****}p < 0.0001$.

See also Figure S1 and Tables S1 and S2.

## RESULTS

### Characterization of Microbiota Colonizing Human Leishmaniasis Lesions and Skin

Dysbiosis in skin microbiota is often associated with inflammation and disease (Grice et al., 2010; Kobayashi et al., 2015; Kong et al., 2012; Oh et al., 2013), suggesting that cutaneous lesions in leishmaniasis might also exhibit changes in the skin-residing bacterial communities. To test this, we analyzed the microbiota of 44 patients infected with *L. braziliensis* (72.7% male, 27.3% female; median age, 27 years old), with lesions present at various body sites (Table S1). We collected two to three skin swabs for each patient, including the lesion, adjacent skin near the lesion, and unaffected contralateral skin of the same body site as the lesion (Figure 1A). Taxonomic composition of unaffected contralateral skin fell within the normal range of what has been previously observed of the healthy skin microbiome, and colonizing microbiota was assessed with respect to gender and no significant differences were found (Meisel et al., 2016; Figure S1A). Bacterial diversity was significantly lower in lesions compared to unaffected contralateral skin and adjacent skin sites, as measured by the observed species-level operational taxonomic units (OTUs) and Shannon diversity indices (Figure 1B).

Interestingly, the skin microbiota on the adjacent skin sites appeared more similar in composition to the lesions than to the contralateral skin (Figure S1A). To quantify the similarity between each site where specimens were collected, we used the Bray-Curtis dissimilarity metric of shared microbial community structure.

*L. major* infection. To test this, we utilized a mouse model of cutaneous leishmaniasis and found that infection with *L. major* changed the skin microbiota in a manner dependent on disease severity. Leishmania-induced dysbiosis was not confined to the site of infection, but occurred globally on the skin of infected mice and, moreover, was transferred to uninfected co-housed mice. Colonization of skin with *Staphylococcus xylosus* isolated from the dysbiotic mice increased inflammatory responses in a contact hypersensitivity model, although not in normal skin, indicating that dysbiosis might exacerbate disease. Dysbiotic microbiota, when transferred to naive mice prior to leishmania infection, increased disease pathology compared to control animals. Taken together, these results indicate that the skin microbiota influences the inflammatory response in leishmaniasis and other inflammatory skin conditions. This work has significant implications for the treatment of cutaneous leishmaniasis and other skin diseases, and highlights the potential of the skin microbiota as a therapeutic target.

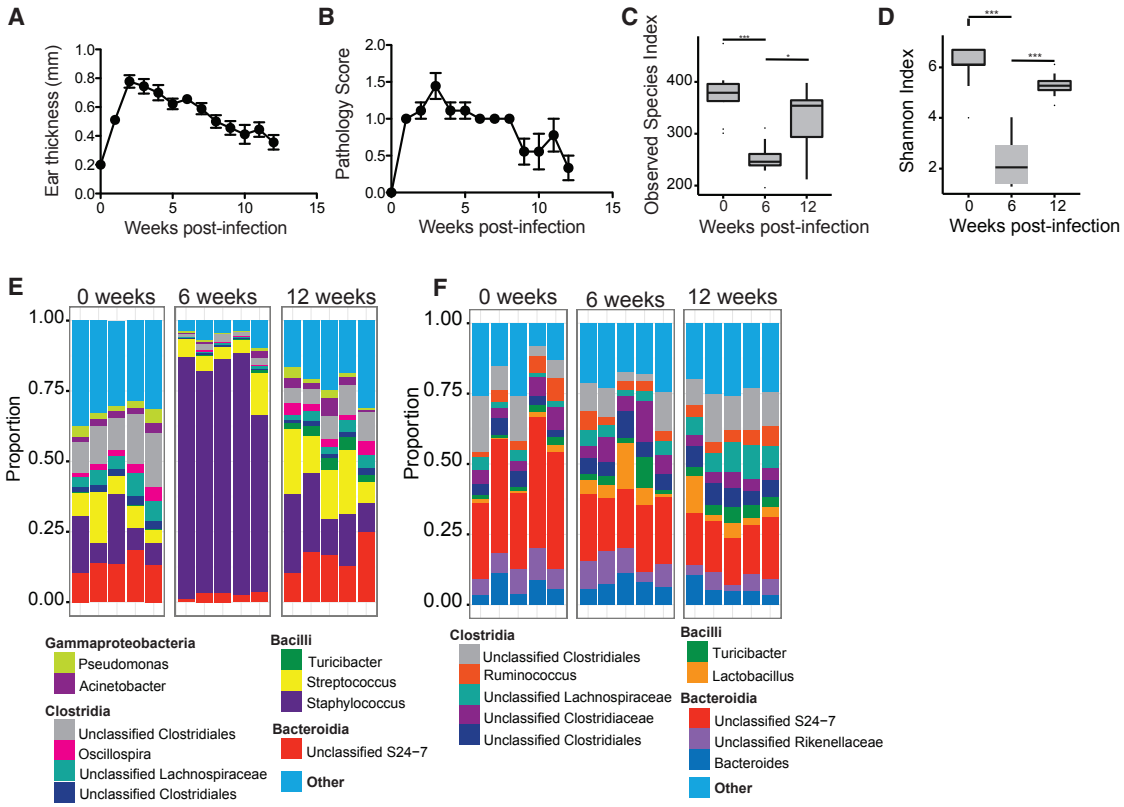


**Figure 2. *L. major* Infection Alters the Skin Microbiota**

C57BL/6 mice were intradermally infected in the ear with $2 \times 10^6$ *L. major* parasites.

(A and B) Lesion size (A) and pathology (B) were assessed over 12 weeks of infection. Data are presented as mean ± SEM.

(C and D) Swabs were collected from the ear at 0, 6, and 12 weeks post-infection and bacterial diversity was assessed by (C) number of observed species-level OTUs and (D) Shannon index. Data are presented as median and IQR as in Figure 1B.

(E and F) Stacked bar charts represent the proportion of the top ten taxa present (E) from ear swabs and (F) from fecal pellets at 0, 6, and 12 weeks post-infection. Each column represents the proportion of taxa for an individual mouse. Data represent two independent experiments (n = 1 skin swab each from 15 mice and n = 1 fecal pellet each from 10 mice). *$p < 0.05$; ***$p < 0.001$.

We observed that lesion and adjacent skin shared greater microbial community structure compared to contralateral and adjacent skin (Figure 1C). These data suggest that microbiota colonizing the lesion is shared with adjacent skin sites, which may have implications in the immune responses at those sites.

We then applied a Dirichlet multinomial mixture model-based approach to assign the lesions to different community types (CTs) based on their taxonomic composition. Lesions clustered into three CTs (Figures 1D and S1B) with distinct bacterial compositions. The top discriminating taxa in CT1 was *Staphylococcus aureus*, CT2 displayed a heterogeneous composition with no dominating taxa, and CT3 was dominated by an unclassified species of *Streptococcus* (Figure 1E; Table S2). These results suggest that cutaneous leishmaniasis lesions are colonized with microbiota similar to other cutaneous ulcers (Kong et al., 2012; Oh et al., 2013; Loesche et al., 2017), but display less heterogeneity of the colonizing microbiota, which is driven primarily by proportions of *Staphylococcus aureus* and *Streptococcus* spp. in this cohort. Interestingly, neither bacteria were associated with larger lesion sizes (Figure S1C), but lesion size may not be a good predictor of disease severity or outcome. Additional epidemiologic studies may be needed to further evaluate the influence of the skin microbiota in cutaneous leishmaniasis, yet these results clearly demonstrate that infection with leishmania alters the skin microbiota, creating several types of dysbiosis.

## *L. major* Infection Induces Changes to the Skin Microbiota in Mouse Models

Since the influence on disease of a dysbiosis is difficult to evaluate in humans, we employed a mouse model of leishmaniasis to assess the role dysbiosis might play in cutaneous leishmaniasis. C57BL/6 mice were infected in the ear with *L. major* parasites, which led to the development of a lesion that resolved by 12 weeks post-infection (Figures 2A and 2B). Prior to infection, and at 6 and 12 weeks post-infection, swabs were collected from the ventral and dorsal ear skin and sequencing of the 16S ribosomal RNA gene was employed to assess skin microbial diversity and composition. Alpha diversity, as measured by the number of observed species-level OTUs and Shannon diversity indices, decreased at 6 weeks post-infection, but returned to pre-infection levels upon lesion resolution (Figures 2C and 2D). This shift in alpha diversity was paralleled by a significant increase in the relative abundance of *Staphylococcus* spp. after lesion development that returned to pre-infection levels once

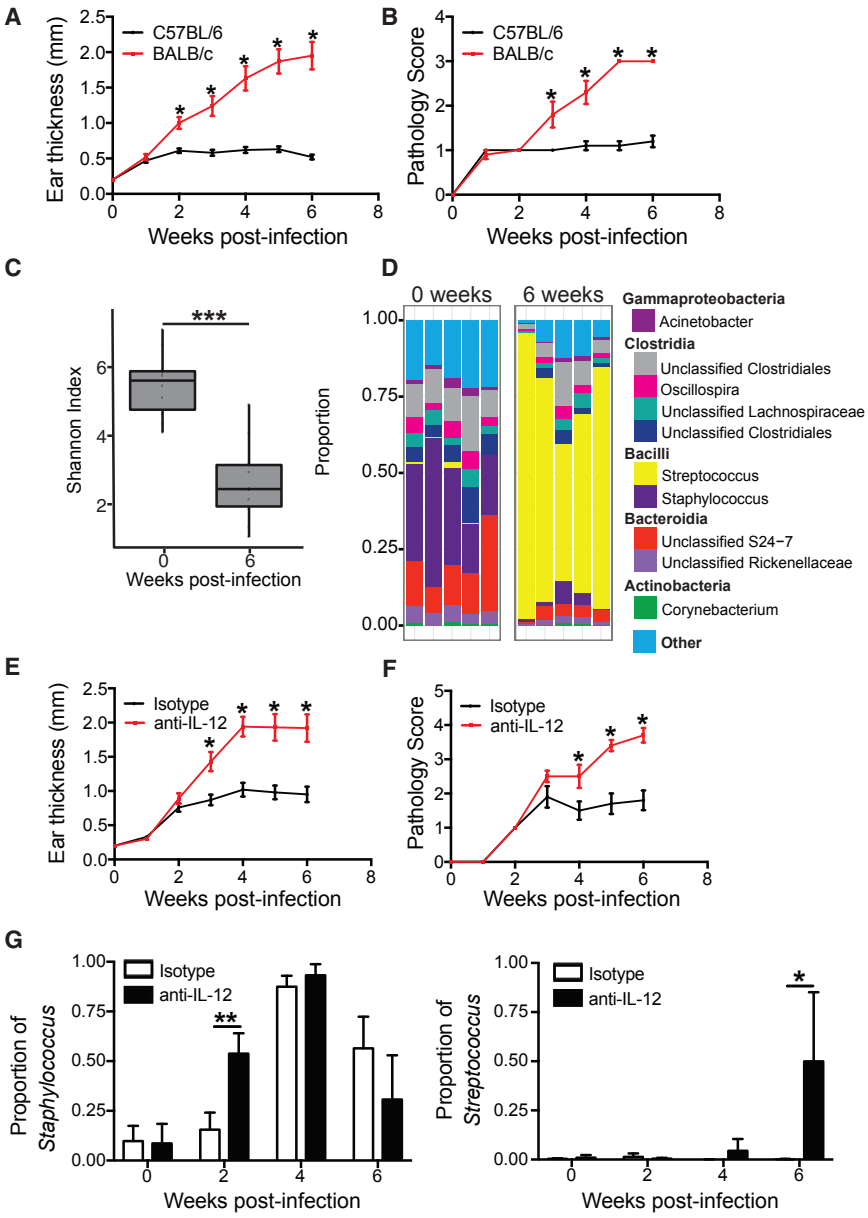


**Figure 3. Skin Microbiota Alterations in *L. major* Infection Are Dependent on Disease Severity**

C57BL/6 and BALB/c mice were intradermally infected with *L. major* parasites.

(A and B) Lesional severity was assessed by (A) ear thickness and (B) a pathology score over the course of infection. Swabs for sequencing of 16S rRNA genes were collected from the lesions at 0 and 6 weeks post-infection.

(C) Alpha diversity was assessed by Shannon index. Data are presented as median and IQR as in Figure 1B.

(D) Stacked bar charts represent the proportion of the top ten taxa present in each sample. Data are representative of two independent experiments (n = 1 skin swab each from 10 mice in each group).

C57BL/6 mice were treated with an isotype or anti-IL-12 mAb and intradermally infected in the ear with *L. major* parasites.

(E and F) Lesional severity was assessed by (E) ear thickness and (F) a pathology score over the course of infection. Anti-IL-12 mAb-treated mice were euthanized at 6 weeks post-infection due to severe disease.

(G) Swabs were collected from the lesions at 2, 4, and 6 weeks post-infection and proportions of *Staphylococcus* and *Streptococcus* were assessed. Data are representative of two independent experiments (n = 1 skin swab each from 10 mice in each group). *p < 0.05; **p < 0.01.

In (A), (B), and (E)–(G), data are presented as mean ± SEM. See also Figure S2.

the lesions resolved (Figure 2E). Speciation of the *Staphylococcus* species associated with *L. major* infection was performed by biochemical typing in an automated system (Microscan, Beckman Coulter) and isolates were identified as *S. xylosus*, a common commensal bacteria found on mouse skin (Nagase et al., 2002). Isolates were then confirmed as *S. xylosus* by MALDI-TOF mass spectrometry using the Bruker MALDI Biotyper System (Beckman Coulter). The MALDI-TOF identification score for all isolates tested was >2.299, which indicates a secure genus identification and a highly probable species identification. Since infections can often lead to changes in the intestinal microbiota (Kamdar et al., 2016; Lozupone et al., 2013), we also analyzed the fecal microbiota of infected mice, but found no significant changes in the fecal bacterial populations throughout the course of infection with *L. major* (Figure 2F), demonstrating that dysbiosis caused by infection is localized to the skin.

## *L. major*-Induced Dysbiosis Differs Depending on the Severity of the Disease

Inflammatory responses induced by a variety of skin insults lead to changes in the skin microbiota (Grice et al., 2010; Gontcharova et al., 2010; Kong et al., 2012; Oh et al., 2013; Loesche et al., 2017), but whether the magnitude of the insult alters the nature or degree of the dysbiosis is not known. To address this, we compared the microbiota from *L. major*-infected C57BL/6 mice that resolve their infection and BALB/c mice that develop severely ulcerated non-healing lesions (Figures 3A and 3B) (Scott and Novais, 2016). Similar to C57BL/6 mice, BALB/c mice had significantly lower alpha diversity at 6 weeks post-infection (Figure 3C). However, in contrast to the dominance of *Staphylococcus* spp. found on lesions of C57BL/6 mice, BALB/c mice had a dominance of *Streptococcus* spp. at 6 weeks post-infection, (Figure 3D). To rule out the possibility that the increase in *Streptococcus* in non-healing BALB/c mice was due to differences in the mouse strain, we depleted IL-12 in C57BL/6 mice, which leads to non-healing lesions similar to those seen in BALB/c mice (Heinzel et al., 1989; Scharton-Kersten et al., 1995). As expected, anti-IL-12

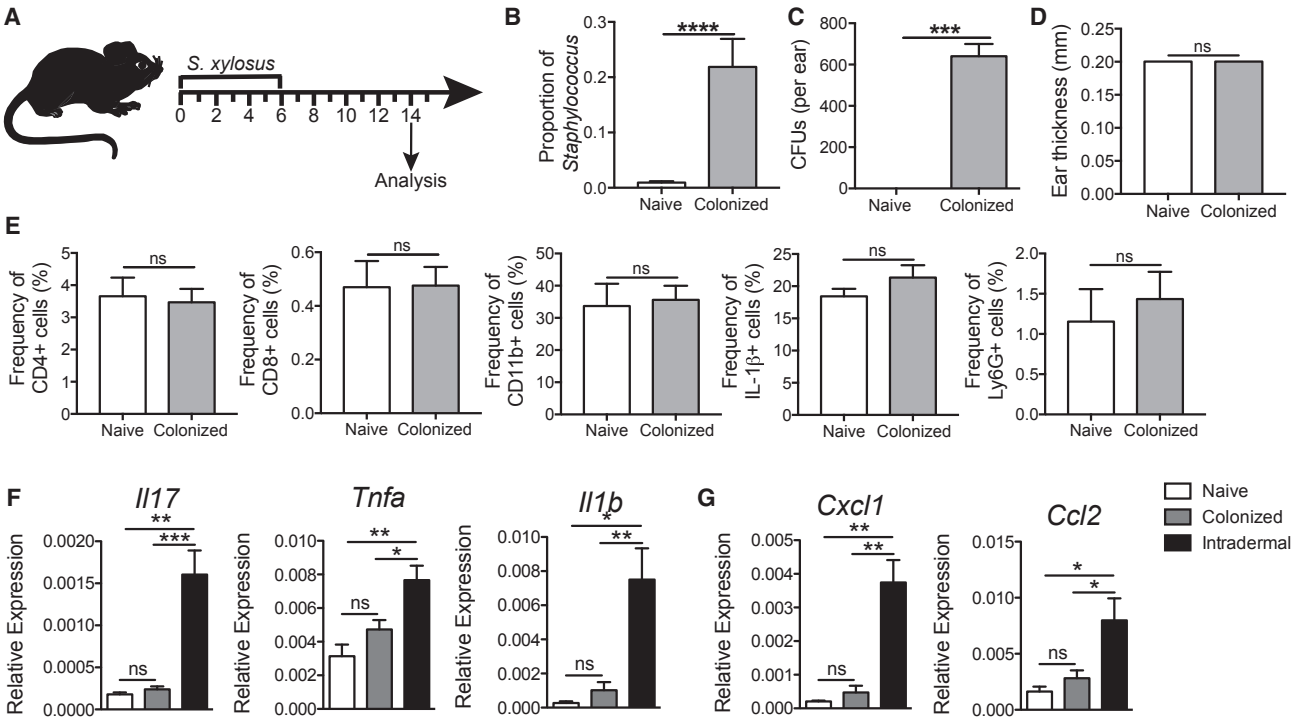


**Figure 4. *Staphylococcus xylosus* Isolated from *L. major* Lesions Causes Inflammation Only When Injected Intradermally**

(A) C57BL/6 mice were topically colonized with $10^8$–$10^9$ *S. xylosus* every other day for a total of four applications; naive mice were unassociated.

(B) Prior to and 14 days post-colonization, swabs were collected to analyze the proportion of *Staphylococcus*.

(C) Ear lysates from naive and *S. xylosus* colonized mice were cultured on mannitol salt agar plates and colony-forming units (CFUs) were counted after overnight incubation at 37°C.

(D) Ear thickness was assessed in naive and colonized mice.

(E) Flow cytometry analysis was performed for the frequency of CD4+; CD8+; and CD11b+, IL-1β+, and Ly6G+ cells in the ears of naive or colonized mice 14 days post-association. Cells were pregated on live, singlet CD45+ cells. Data are representative of two independent experiments (n = 1 ear tissue each from 4 mice in each group). C57BL/6 mice were topically colonized or intradermally infected in the ear with *S. xylosus*.

(F and G) Fourteen days later, skin was harvested and mRNA expression was assessed for (F) cytokine and (G) chemokine genes. Data are representative of one experiment (n = 1 ear tissue each from 5 mice in each group). ns, not significant; *p < 0.05; **p < 0.01; ***p < 0.001; ****p < 0.0001.

In (B)–(G), data are presented as mean ± SEM. See also Figure S3.

mAb-treated mice developed large non-healing lesions (Figures 3E and 3F). We first analyzed the skin microbiota of naive mice treated with anti-IL-12 prior to infection and found that treatment does not significantly alter the proportions of *Staphylococcus* spp. or *Streptococcus* spp. (Figure S2A). However, after 2 weeks of *L. major* infection, *Staphylococcus* spp. made up a high proportion of the skin microbiota in the anti-IL-12-treated mice, while remaining low in the isotype-treated mice until 4 weeks post-infection (Figures 3G and S2B). At 6 weeks post-infection, the relative abundance of *Streptococcus* spp. remained less than 1% of the total population in control mice, but it increased significantly in anti-IL-12-treated mice to >50% relative abundance (Figures 3G and S2B), further demonstrating that *Streptococcus* spp. are associated with more severely ulcerated lesions. Taken together, our data suggest that *L. major* infection elicits severity-dependent changes in the skin microbiota.

## *S. xylosus*-Mediated Inflammation Is Dependent on Tissue Damage

To determine if the dysbiosis caused by *L. major* infection would influence skin inflammatory responses, we topically associated naive mice with *S. xylosus* (Figure 4A). One week following colonization with *S. xylosus*, mice exhibited a significantly higher relative and absolute abundance of *Staphylococcus* spp. compared with naive mice by culture-independent (Figure 4B) and culture-dependent assays (Figure 4C). Interestingly, *S. xylosus* colonization did not influence ear thickness (Figure 4D); the frequency or total cell numbers of CD4+ T cells, CD8+ T cells, and CD11b+ myeloid cells; IL-1β production; Ly6G+ neutrophils (Figures 4E and S3A–S3E); or T cell cytokine production (Figures S3F and S3G). To determine if *S. xylosus* incites inflammation upon breach of the skin barrier, we injected mice intradermally with *S. xylosus* and analyzed the inflammatory response in the skin. These mice had significantly higher expression of *Il17*, *Tnfa*, *Il1b*, *Cxcl1*, and *Ccl2* compared with either naive or colonized mice (Figures 4F and 4G), suggesting that *S. xylosus* might contribute to skin inflammation when the skin barrier is compromised.

While skin colonized with *S. xylosus* appeared immunologically normal, based on the results above we hypothesized that the response to damage might differ between normal and dysbiotic skin. We tested this idea using a model of contact

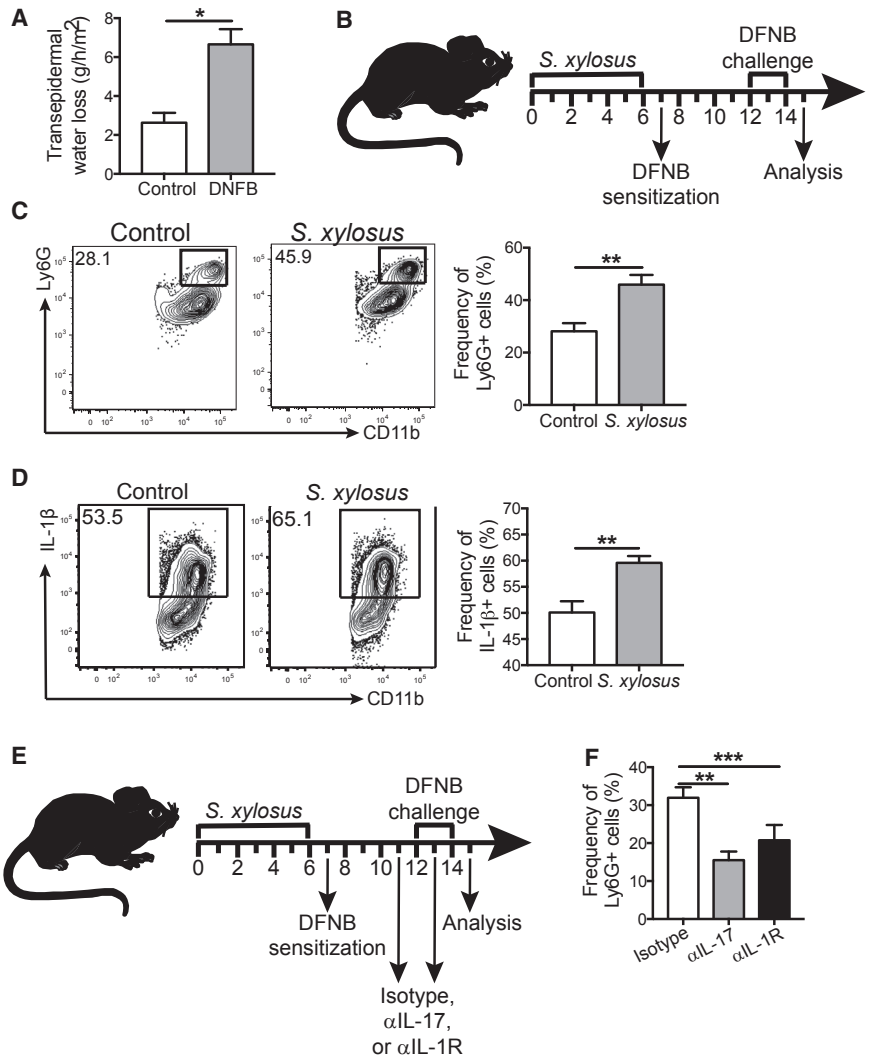


**Figure 5. *S. xylosus* Colonization Exacerbates Skin Inflammation during Contact Hypersensitivity**

(A) C57BL/6 mice were sensitized with DNFB or vehicle control on the belly and challenged with DNFB or vehicle 5 days later. Transepidermal water loss was measured on ear skin of vehicle control and DNFB-treated mice.

(B) C57BL/6 mice were topically associated with $10^8$–$10^9$ *S. xylosus* every other day for a total of four applications and control C57BL/6 mice were left unassociated. The next day, control and *S. xylosus* associated mice were sensitized on the belly with DNFB. Five days later, control and *S. xylosus* associated mice were challenged with DNFB.

(C and D) Representative flow cytometry plots and graphs depict the expression of (C) CD11b+ Ly6G+ cells and (D) CD11b+ IL-1β+ cells.

(E) C57BL/6 mice were topically associated with $10^8$–$10^9$ *S. xylosus* every other day for a total of four applications and then treated with isotype, anti-IL-17, or anti-IL-1R mAbs prior to sensitization and challenge with DNFB.

(F) Graphs depict the expression of CD11b+ Ly6G+ cells in the skin of treated mice. All data are representative of two independent experiments (n = 1 ear tissue each from 5 mice in each group). *p < 0.05; **p < 0.01; ***p < 0.001.

In (A), (C), (D), and (F), data are presented as mean ± SEM. See also Figure S4.

hypersensitivity in which sensitizing and challenging the skin with a known skin irritant, dinitrofluorobenzene (DNFB), increases transepidermal water loss, an indication of skin barrier dysfunction and inflammation (Figure 5A). Naive C57BL/6 mice were colonized with *S. xylosus* prior to sensitization with DNFB (Figure 5B). DNFB challenge resulted in a significant increase in neutrophils (CD11b+ Ly6G+) and expression of pro-IL-1β from myeloid cells (Figures 5C and 5D). A similar immune response was observed when mice were colonized with *S. xylosus* during the challenge phase of DNFB treatment (Figure S4A). Since IL-17 and IL-1 can both lead to an increase in neutrophil recruitment, we investigated whether these cytokines played a role in the increase of neutrophils in *S. xylosus*-treated mice. Mice colonized with *S. xylosus* were treated with an isotype control mAb, anti-IL-17A mAb, or anti-IL-1R mAb prior to DNFB challenge (Figure 5E), and neutralizing IL-17 or IL-1 decreased neutrophil recruitment (Figure 5F). Thus, it appears that a commensal such as *S. xylosus* can induce IL-17 and IL-1 expression in conditions of tissue stress and damage, leading to increased inflammation.

To determine if colonization with *Streptococcus* spp. might have a similar effect, we isolated *Streptococcus* from *L. major*-infected mice that had been treated with anti-IL-12 mAb. The immune responses in mice sensitized and challenged with DNFB colonized with *Streptococcus* were unchanged (Figure S4B). However, we were unable to achieve stable colonization with the streptococcal isolate (Figure S4C), suggesting that this particular lesion-associated *Streptococcus* isolate requires additional, as-yet-undefined nutrients or other conditions to colonize normal skin. We hypothesized that the *Streptococcus* isolate would establish a better colonization on lesional skin; thus, we infected mice with *L. major*, allowed the lesion to develop, and then colonized with the *Streptococcus* isolate. Indeed, *Streptococcus* colonized the lesion better than naive skin (Figure S4D). Interestingly, colonization with the *Streptococcus* isolate did not exacerbate lesion development or the inflammatory response in the skin (Figures S4E and S4F).

## *L. major*-Induced Dysbiosis Is Transmissible to Uninfected Skin

The observation that the lesional microbiota of human cutaneous leishmaniasis extends to adjacent, seemingly normal skin sites prompted us to ask if the same was true in the mouse model of *L. major* infection. To answer this question, we compared the bacterial composition at the lesion site (infected ear) and the contralateral ear of infected mice. As expected, the infected ear was dominated by *Staphylococcus* spp. at the peak of infection. Interestingly, the contralateral

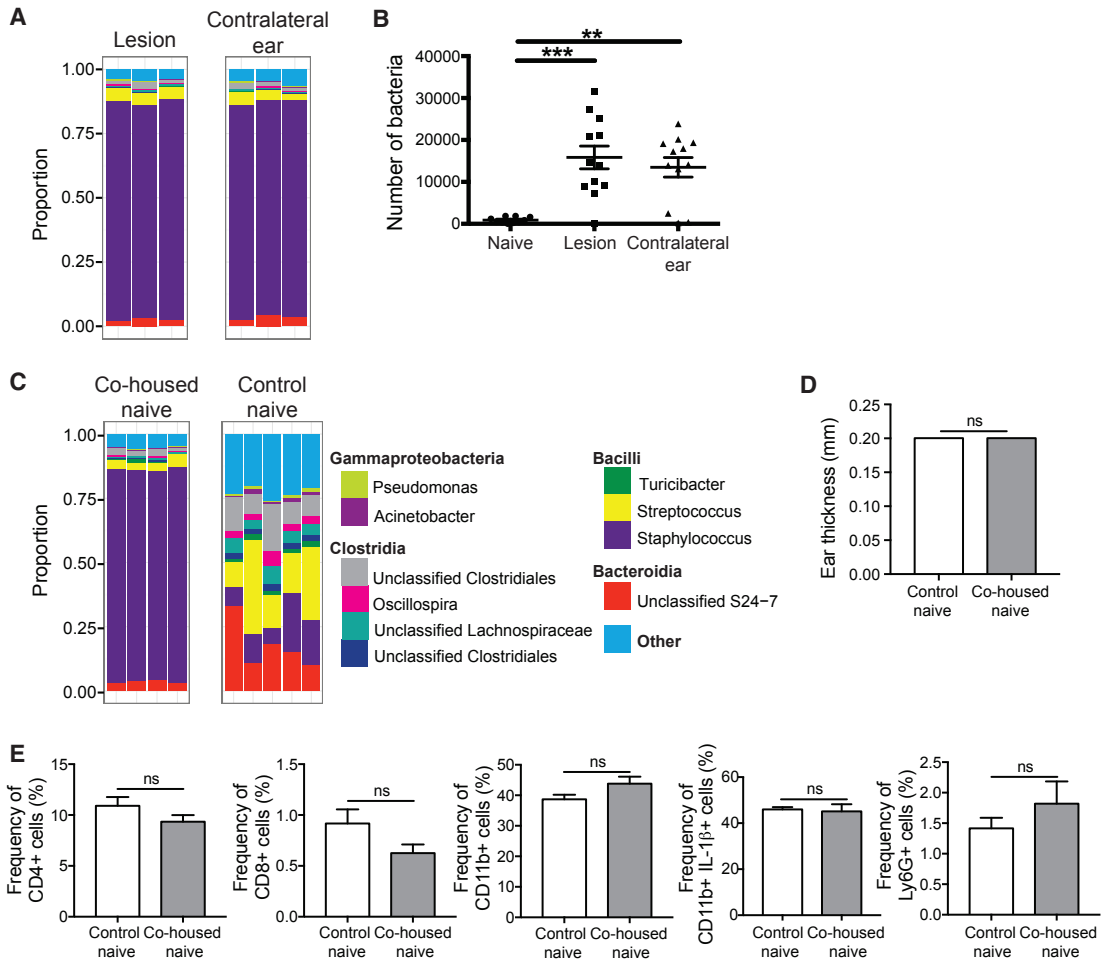


**Figure 6. *L. major*-Induced Dysbiosis Is Transmissible to Uninfected Skin**

(A) C57BL/6 mice were intradermally infected with *L. major* and swabs were collected from the infected and contralateral ears at 6 weeks post-infection for 16S rRNA gene analysis. Stacked bar charts represent the proportion of the top ten taxa present in each sample. Data are representative of three independent experiments (n = 1 swab of each ear from 15 mice).

(B) Swabs from naive or *L. major*-infected C57BL/6 mice were cultured on mannitol salt agar plates and CFUs were counted to determine bacteria burden. Data are representative of one experiment (for naive group, n = 1 swab from the ear of 10 mice; for infected and contralateral ears, n = 1 swab of each ear from 12 mice).

(C) Naive C57BL/6 mice were co-housed with *L. major*-infected mice for 6 weeks, while control naive mice were housed separately. Swabs were collected from co-housed naive and control naive mice. Stacked bar charts represent the proportion of taxa present in each sample. Data are representative of two independent experiments (for infected group, n = 1 swab of each ear from 15 mice; for co-housed naive, n = 1 swab of one ear from 10 mice; for control naive, n = 1 swab of one ear from 5 mice).

(D) Bar graphs depict ear thickness of control and co-housed naive mice.

(E) Cells were isolated from the ears of co-housed naive mice and control naive mice to assess for CD4+; CD8+; and CD11b+, IL-1β+, and Ly6G+ cells by flow cytometry. Data are representative of one experiment (co-housed naive, n = 1 ear tissue each from 4 mice; control naive, n = 1 ear tissue each from 5 mice). ns, not significant; $^{**}p < 0.01$; $^{***}p < 0.001$.

In (B), (D), and (E), data are presented as mean ± SEM. See also Figure S5.

ear also had a high proportion of *Staphylococcus* spp., despite the absence of infection (Figure 6A). We also observed higher bacterial loads on the infected and contralateral ears when compared to naive skin (Figure 6B). These data demonstrate that in the mouse model, the dysbiotic microbiota caused by *L. major* infection is transmissible to the non-inflamed, contralateral ear.

A dysbiotic intestinal microbiota is often transmissible by simply co-housing mice (Elinav et al., 2011; Zenewicz et al., 2013). Whether transmission of the skin microbiota also occurs is less clear, although co-habiting families may share their skin microbiota (Song et al., 2013). To directly address this issue, we tested if naive mice co-housed with *L. major*-infected mice might acquire their dysbiotic microbiota. C57BL/6 mice were infected with *L. major* and co-housed with naive mice for 6 weeks, while a group of control naive mice were housed separately. Similar to the infected and contralateral ears, the skin of the co-housed naive mice also acquired a high abundance of *Staphylococcus* spp., while the control naive mice maintained a diverse population of bacteria (Figure 6C). Similar to what we observed with

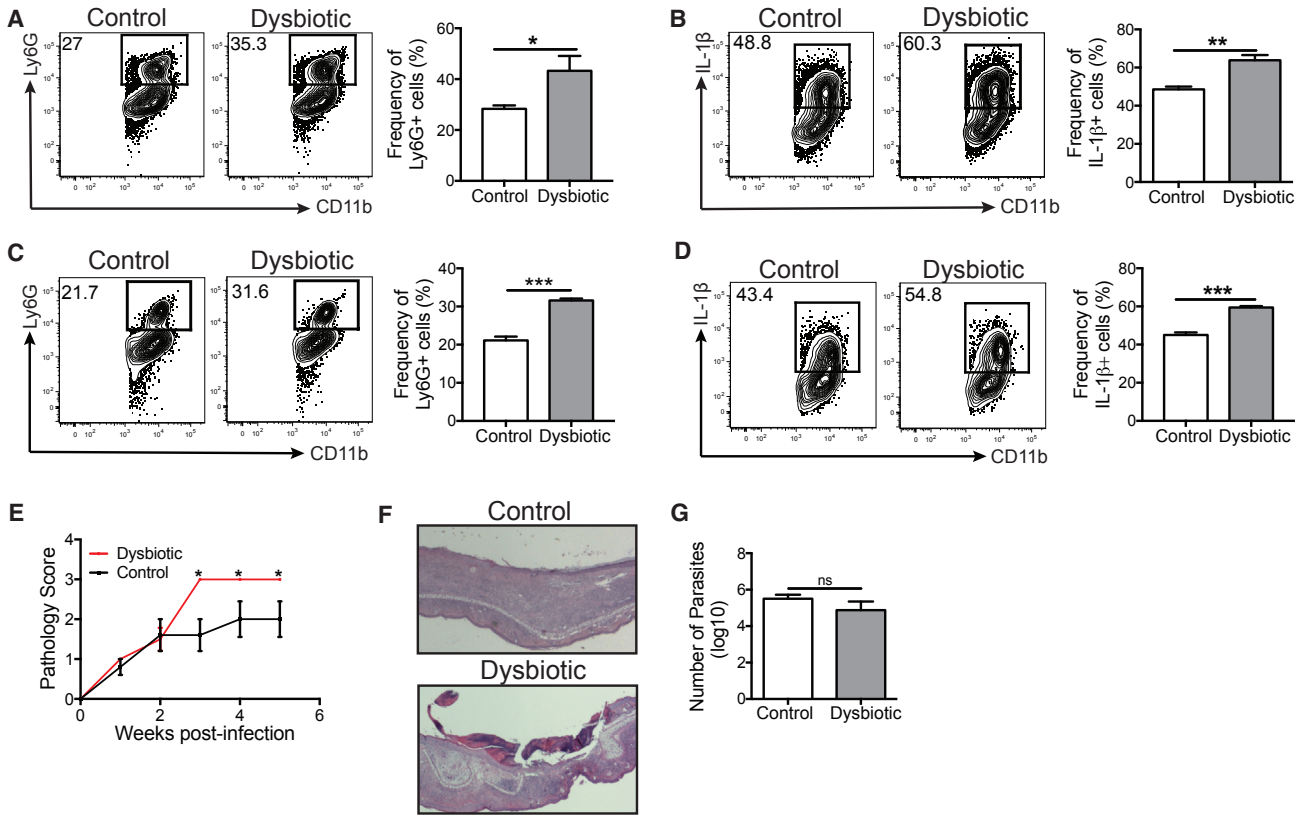


**Figure 7. Dysbiosis Exacerbates Inflammation during DNFB Treatment and *L. major* Infection**

Naive C57BL/6 mice acquired dysbiotic microbiota after co-housing with *L. major*-infected mice for 6 weeks. Control and dysbiotic mice were then sensitized and challenged with DNFB.

(A and B) Representative flow cytometry plots and graphs of skin cells depict the expression of (A) CD11b+ Ly6G+ cells and (B) CD11b+ IL-1β+ cells. Control and dysbiotic mice were intradermally infected with *L. major* parasites and the cells from the lesions were collected at 5 weeks post-infection.

(C and D) Representative flow cytometry plots and graphs of skin cells depict the expression of (C) CD11b+ Ly6G+ cells and (D) CD11b+ IL-1β+ cells.

(E) A pathology score was used to assess disease severity over 5 weeks post-infection.

(F) Representative ear skin sections stained with hemotoxylin and eosin of *L. major*-infected control and dysbiotic mice.

(G) Parasite burdens were assessed using a limiting dilution assay after 5 weeks post-infection. Data are representative of two independent experiments (for dysbiotic group, n = 1 ear tissue each from 4 mice; for control group, n = 1 ear tissue each from 5 mice). ns, not significant; *p < 0.05; **p < 0.01; ***p < 0.001. Data are presented as mean ± SEM.

*S. xylosus* colonized mice, the ear thickness and immune response in co-housed naive mice were not altered by dysbiosis (Figures 6D, 6E, and S5). Our data demonstrate that the dysbiotic skin microbiota caused by *L. major* infection is transmissible to naive mice without causing inflammation. This model allows us to assess the consequences of dysbiosis in inflammatory responses occurring in the skin.

### *L. major*-Induced Dysbiosis Exacerbates Disease during Inflammation and Infection

While we and others have shown that colonizing mice with a single organism at high levels can alter immune responses (Figure 5) (Naik et al., 2012, 2015), whether a naturally transmitted dysbiosis would alter skin immune responses has not been tested. To assess this, we co-housed naive mice with *L. major*-infected mice for 6 weeks to create naive dysbiotic mice. Control mice were housed separately and never exposed to *L. major*-infected mice. We then compared the contact hypersensitivity responses of both groups of mice to DNFB. Dysbiotic co-housed mice had significantly more neutrophils and pro-IL-1β production in the skin than control mice (Figures 7A and 7B), similar to mice colonized with high numbers of bacteria.

Taken together, our results suggested that mice with dysbiotic skin might respond differently to infection with *L. major* when compared with normal mice. To determine if this was the case, naive mice were co-housed with *L. major*-infected mice for 6 weeks and then infected with *L. major*. At 5 weeks post-infection, we analyzed the inflammatory cells and cytokines in the lesions of control and dysbiotic mice. Similar to DNFB challenge, *L. major*-infected skin had significantly more neutrophils and IL-1β in dysbiotic mice compared to control mice (Figures 7C and 7D). Furthermore, the dysbiotic mice had significantly greater lesion severity, characterized by increased skin ulceration, than control mice (Figures 7E and 7F), despite similar parasite burdens (Figure 7G). These findings demonstrate that the skin microbiota influences the magnitude of lesion severity following infection with *L. major*.

## DISCUSSION

Interactions between the immune system and the microbiota can be either beneficial or harmful, depending on the context (Gaboriau-Routhiau et al., 2009; Naik et al., 2012, 2015; Atarashi et al., 2013; Kobayashi et al., 2015). In our studies, we found that leishmania infections in humans and mice change the composition of the skin microbiota. The nature of the changes in mice differed depending on the severity of inflammation, with *Staphylococcus* spp. dominant in moderate lesions and *Streptococcus* spp. increasing in more severe lesions in mice infected with *L. major*. In humans, we found individuals with a dominance of *Staphylococcus aureus*, *Streptococcus* spp., or a mixture of both, although whether these distinct skin microbiota influence the outcome of disease is yet unknown. However, our studies in mice clearly suggest that further studies in patients are warranted.

Why dysbiosis occurs during cutaneous leishmaniasis, or in other inflammatory conditions, is unknown. Innate defenses, such as antimicrobial peptides (AMPs), can target certain bacteria and play a role in disrupting the microbiota in the intestine and in the skin (Cogen et al., 2010; Dorschner et al., 2001; Natsuga et al., 2016; Nizet et al., 2001; Salzman et al., 2010), and may also in part contribute to the dysbiosis caused by *L. major* infection. We found that infection with *L. major* causes changes in AMP expression in the skin (Figure S6), and mice deficient in a cathelicidin-type antimicrobial peptide (CAMP) appear more susceptible to infection with *L. amazonensis* (Kulkarni et al., 2006). Whether this deficiency in CAMP causes changes in the skin microbiota remains to be determined, but these results, in addition to our own findings, suggest that AMPs in cutaneous leishmaniasis warrant further investigation. How AMPs might promote these changes is unclear, but virulence factors can make bacteria resistant to AMPs, and both *Staphylococcus* spp. and *Streptococcus* spp. express genes that protect them from AMP killing (Kristian et al., 2005; Peschel et al., 1999, 2001), potentially providing them with a survival advantage during *L. major* infection.

One difficulty in studying the microbiota is assessing how changes in the skin microbiota influence disease, since skin dysbiosis is the consequence of the inflammatory response in the skin. While transmissibility of dysbiotic microbiota has been demonstrated in the intestinal tract (Elinav et al., 2011; Zenewicz et al., 2013), our data demonstrate transmissibility of the skin microbiota in a murine model. In this study and previous studies, colonization with a single bacterial species enhanced skin inflammation (Naik et al., 2012). In our studies, enhanced inflammation was only observed when there was pre-existing tissue damage and inflammation. The differences between these studies are likely due to differences in bacterial species. Although mono-colonization will be essential for dissecting how particular bacteria alter immune responses, it will not replicate the complex changes that might be associated with a naturally occurring dysbiosis. Our ability to generate a mouse with dysbiotic skin microbiota overcomes this issue, and has allowed us to demonstrate that a naturally acquired dysbiosis promotes increased inflammatory responses and, in the case of cutaneous leishmaniasis, increased disease. It is not clear how this transmission occurs, although consistent with our results, evidence from human studies indicates that the environment influences the skin microbiota (Song et al., 2013), and *L. major* infections in mice may provide a model to study the mechanisms involved.

The findings from our mouse model of cutaneous leishmaniasis are similar to the dysbiosis that occurs during human cutaneous leishmaniasis. Interestingly, the different topological sites of our samples did not show any differences in the skin microbiota, although we only had a few samples from moist and sebaceous sites. Yet comparable to what has been reported by culture-dependent and culture-independent methods (Isaac-Márquez and Lezama-Dávila, 2003; Sadeghian et al., 2011; Layegh et al., 2015; Salgado et al., 2016), our results demonstrated that *Staphylococcus aureus* and an unclassified species of *Streptococcus* are highly abundant on lesional skin. This dysbiosis was also present on skin sites adjacent to the lesion. However, unlike our mouse model, the dysbiotic skin microbiota did not appear to be transmissible to contralateral skin sites. It is not yet clear why the dysbiosis is confined to the lesional and adjacent skin sites in human cutaneous leishmaniasis, but it is likely to be due to differences in grooming and environmental conditions between mice and humans. However, the similarities in the dysbiotic microbiota between the mouse model and human cutaneous leishmaniasis demonstrate the utility of our model system to study the role of skin microbiota during leishmania infections.

One of our findings was that skin dysbiosis does not cause immunologic changes in the skin or disease by itself, nor did topical colonization with *S. xylosus*. However, in mice where tissue stress is induced by contact hypersensitivity to DNFB, *S. xylosus* exacerbated the inflammatory response, assessed by increased recruitment of neutrophils and upregulated expression of IL-1β. These results are consistent with other studies showing that mice with barrier defects allow *Staphylococcus* to penetrate the epidermal barrier and subsequently increase cytokine expression in the skin (Nakatsuji et al., 2016). In some situations, the cytokine production may be protective, such as during a fungal infection (Naik et al., 2015). However, in cutaneous leishmaniasis, neutrophils and IL-1β are associated with increased pathology rather than the restriction of parasites (Charmoy et al., 2016; Fernández-Figueroa et al., 2012; Gimblet et al., 2015; Gonzalez-Lombana et al., 2013; Novais et al., 2015; Voronov et al., 2010). Thus, we hypothesize that *L. major* infection disturbs skin barrier integrity while simultaneously inducing a dysbiosis in the skin microbiota, which taken together lead to the increased recruitment of neutrophils and IL-1β recruiting cells to the skin, and cause increased lesion severity.

These results raise the obvious question of what role systemic or topical antibiotics might play in moderating inflammatory responses associated with leishmaniasis (Grice, 2014). As previous studies with germ-free mice indicate that commensal bacteria may contribute to lesion severity in cutaneous leishmaniasis (de Oliveira et al., 1999; Naik et al., 2012; Oliveira et al., 2005), and our studies demonstrate that dysbiosis exacerbates disease, it is reasonable to predict that antibiotic treatment might be beneficial in leishmaniaisis. While we have been unsuccessful in moderating disease in mice by antibiotic treatment, there are examples of antibiotic therapy being protective in some cutaneous leishmaniasis patients (Aguiar et al., 2010; Ben Salah et al., 2013; Kim et al., 2009; Krolewiecki et al., 2002). However,

there are other studies that find no effect of antibiotic treatment (Iraji and Sadeghinia, 2005; Neva et al., 1997), and moreover, when such treatment shows a positive outcome the mechanism involved is not clear. Given the different outcomes of studies looking at antibiotic treatment, and taken together with our results, it appears that the role of antibiotics in treatment needs further investigation.

In summary, our findings indicate that the skin microbiota not only changes during leishmania infection, but also when transmitted to naive mice can enhance disease to leishmania. These findings have obvious consequences when considering how to limit disease severity in cutaneous leishmaniasis. Moreover, since we find that the dominant bacteria associated with a leishmania-induced dysbiosis differ depending upon the severity of disease in mice, further epidemiologic studies with patients to determine the consequences of differing types of dysbiosis are warranted. Finally, we found that dysbiotic skin microbiota can be transmitted to conventional naive mice, which provides a model to define how and when dysbiosis might influence control of other infections, autoimmune diseases, and wound healing.

## STAR★METHODS

Detailed methods are provided in the online version of this paper and include the following:

- KEY RESOURCES TABLE
- CONTACT FOR REAGENT AND RESOURCE SHARING
- EXPERIMENTAL MODEL AND SUBJECT DETAILS
  - Mice
  - Human Cutaneous Leishmaniasis Subjects
  - Parasite and Bacterial Cultures
- METHOD DETAILS
  - Leishmania Infection and In Vivo Antibody Depletions
  - Bacterial Topical Associations, Intradermal Infections, and CFU Quantification
  - Contact Hypersensitivity and Antibody Treatments
  - Preparation of Dermal Sheets
  - Antibodies and Flow Cytometry
  - RNA Isolation, Purification, and Quantitative Real-Time PCR
  - Microbiota Collection, Sequencing, and Analysis
- QUANTIFICATION AND STATISTICAL ANALYSIS
  - Pre-processing and Community Characterization of 16S rRNA Sequence Data
  - Sample Sizes
  - Statistical Analysis
- DATA AND SOFTWARE AVAILABILITY

### SUPPLEMENTAL INFORMATION

Supplemental Information includes six figures and three tables and can be found with this article online at http://dx.doi.org/10.1016/j.chom.2017.06.006.

### AUTHOR CONTRIBUTIONS

Conceptualization, C.G., P.S., E.M.C., and E.A.G.; Methodology, C.G., P.S., and E.A.G.; Validation, C.G.; Formal Analysis, C.G., J.S.M., and M.A.L.; Investigation, C.G., S.D.C., J.H., F.O.N., C.W.B., and A.M.M.; Resources, P.S., E.A.G., S.C.R., L.P.C., E.M.C., D.P.B., and C.W.B.; Data Curation, C.G., J.S.M., F.O.N., L.P.C., and E.M.C.; Writing – Original Draft, C.G., P.S., and E.A.G.; Writing – Review & Editing, C.G., J.S.M., M.A.L., S.D.C., J.H., F.O.N., A.M.M., C.W.B., D.P.B., S.C.R., L.P.C., E.M.C., P.S., and E.A.G.; Visualization, C.G. and J.S.M.; Supervision, P.S. and E.A.G.; Funding Acquisition, P.S., E.A.G., and E.M.C.

### ACKNOWLEDGMENTS

Research was funded by grants from the NIH: F31 AI 114227 to C.G., RO1 AI 1068432 and U01 AI088650 to P.S., R00AR060873 and R01AR066663 to E.A.G., and P50 AI030639 to E.M.C. Funding was also provided by the Penn-Chop Microbiome Program. The content is solely the responsibility of the authors and does not necessarily represent the official views of the NIH. The authors would like to thank Ba Nguyen for technical assistance with experiments, as well as the laboratory of Dr. Yasmine Belkaid (NIAID, LPD, NIH) for bacterial isolate sequencing and identification.

Received: February 19, 2017
Revised: May 9, 2017
Accepted: June 8, 2017
Published: June 29, 2017

### REFERENCES

Aguiar, M.G., Pereira, A.M., Fernandes, A.P., and Ferreira, L.A. (2010). Reductions in skin and systemic parasite burdens as a combined effect of topical paromomycin and oral miltefosine treatment of mice experimentally infected with Leishmania (Leishmania) amazonensis. Antimicrob. Agents Chemother. *54*, 4699–4704.

Antonelli, L.R., Dutra, W.O., Almeida, R.P., Bacellar, O., Carvalho, E.M., and Gollob, K.J. (2005). Activated inflammatory T cells correlate with lesion size in human cutaneous leishmaniasis. Immunol. Lett. *101*, 226–230.

Atarashi, K., Tanoue, T., Oshima, K., Suda, W., Nagano, Y., Nishikawa, H., Fukuda, S., Saito, T., Narushima, S., Hase, K., et al. (2013). Treg induction by a rationally selected mixture of Clostridia strains from the human microbiota. Nature *500*, 232–236.

Ben Salah, A., Ben Messaoud, N., Guedri, E., Zaatour, A., Ben Alaya, N., Bettaieb, J., Gharbi, A., Belhadj Hamida, N., Boukthir, A., Chlif, S., et al. (2013). Topical paromomycin with or without gentamicin for cutaneous leishmaniasis. N. Engl. J. Med. *368*, 524–532.

Canesso, M.C., Vieira, A.T., Castro, T.B., Schirmer, B.G., Cisalpino, D., Martins, F.S., Rachid, M.A., Nicoli, J.R., Teixeira, M.M., and Barcelos, L.S. (2014). Skin wound healing is accelerated and scarless in the absence of commensal microbiota. J. Immunol. *193*, 5171–5180.

Caporaso, J.G., Kuczynski, J., Stombaugh, J., Bittinger, K., Bushman, F.D., Costello, E.K., Fierer, N., Peña, A.G., Goodrich, J.K., Gordon, J.I., et al. (2010). QIIME allows analysis of high-throughput community sequencing data. Nat. Methods *7*, 335–336.

Charmoy, M., Hurrell, B.P., Romano, A., Lee, S.H., Ribeiro-Gomes, F., Riteau, N., Mayer-Barber, K., Tacchini-Cottier, F., and Sacks, D.L. (2016). The Nlrp3 inflammasome, IL-1β, and neutrophil recruitment are required for susceptibility to a nonhealing strain of Leishmania major in C57BL/6 mice. Eur. J. Immunol. *46*, 897–911.

Cogen, A.L., Yamasaki, K., Sanchez, K.M., Dorschner, R.A., Lai, Y., MacLeod, D.T., Torpey, J.W., Otto, M., Nizet, V., Kim, J.E., and Gallo, R.L. (2010). Selective antimicrobial action is provided by phenol-soluble modulins derived from Staphylococcus epidermidis, a normal resident of the skin. J. Invest. Dermatol. *130*, 192–200.

Crosby, E.J., Goldschmidt, M.H., Wherry, E.J., and Scott, P. (2014). Engagement of NKG2D on bystander memory CD8 T cells promotes increased immunopathology following Leishmania major infection. PLoS Pathog. *10*, e1003970.

de Oliveira, M.R., Tafuri, W.L., Nicoli, J.R., Vieira, E.C., Melo, M.N., and Vieira, L.Q. (1999). Influence of microbiota in experimental cutaneous leishmaniasis in Swiss mice. Rev. Inst. Med. Trop. Sao Paulo *41*, 87–94.

Dorschner, R.A., Pestonjamasp, V.K., Tamakuwala, S., Ohtake, T., Rudisill, J., Nizet, V., Agerberth, B., Gudmundsson, G.H., and Gallo, R.L. (2001). Cutaneous injury induces the release of cathelicidin anti-microbial peptides active against group A Streptococcus. J. Invest. Dermatol. *117*, 91–97.

Edgar, R.C. (2010). Search and clustering orders of magnitude faster than BLAST. Bioinformatics *26*, 2460–2461.

Elinav, E., Strowig, T., Kau, A.L., Henao-Mejia, J., Thaiss, C.A., Booth, C.J., Peaper, D.R., Bertin, J., Eisenbarth, S.C., Gordon, J.I., and Flavell, R.A. (2011). NLRP6 inflammasome regulates colonic microbial ecology and risk for colitis. Cell *145*, 745–757.

Fernández-Figueroa, E.A., Rangel-Escareño, C., Espinosa-Mateos, V., Carrillo-Sánchez, K., Salaiza-Suazo, N., Carrada-Figueroa, G., March-Mifsut, S., and Becker, I. (2012). Disease severity in patients infected with Leishmania mexicana relates to IL-1β. PLoS Negl. Trop. Dis. *6*, e1533.

Gaboriau-Routhiau, V., Rakotobe, S., Lécuyer, E., Mulder, I., Lan, A., Bridonneau, C., Rochet, V., Pisi, A., De Paepe, M., Brandi, G., et al. (2009). The key role of segmented filamentous bacteria in the coordinated maturation of gut helper T cell responses. Immunity *31*, 677–689.

Gimblet, C., Loesche, M.A., Carvalho, L., Carvalho, E.M., Grice, E.A., Artis, D., and Scott, P. (2015). IL-22 protects against tissue damage during cutaneous leishmaniasis. PLoS One *10*, e0134698.

Gontcharova, V., Youn, E., Sun, Y., Wolcott, R.D., and Dowd, S.E. (2010). A comparison of bacterial composition in diabetic ulcers and contralateral intact skin. Open Microbiol. J. *4*, 8–19.

Gonzalez-Lombana, C., Gimblet, C., Bacellar, O., Oliveira, W.W., Passos, S., Carvalho, L.P., Goldschmidt, M., Carvalho, E.M., and Scott, P. (2013). IL-17 mediates immunopathology in the absence of IL-10 following Leishmania major infection. PLoS Pathog. *9*, e1003243.

Grice, E.A. (2014). The skin microbiome: potential for novel diagnostic and therapeutic approaches to cutaneous disease. Semin. Cutan. Med. Surg. *33*, 98–103.

Grice, E.A., Snitkin, E.S., Yockey, L.J., Bermudez, D.M., Liechty, K.W., and Segre, J.A.; NISC Comparative Sequencing Program (2010). Longitudinal shift in diabetic wound microbiota correlates with prolonged skin defense response. Proc. Natl. Acad. Sci. USA *107*, 14799–14804.

Hannigan, G.D., Hodkinson, B.P., McGinnis, K., Tyldsley, A.S., Anari, J.B., Horan, A.D., Grice, E.A., and Mehta, S. (2014). Culture-independent pilot study of microbiota colonizing open fractures and association with severity, mechanism, location, and complication from presentation to early outpatient follow-up. J. Orthop. Res. *32*, 597–605.

Heinzel, F.P., Sadick, M.D., Holaday, B.J., Coffman, R.L., and Locksley, R.M. (1989). Reciprocal expression of interferon gamma or interleukin 4 during the resolution or progression of murine leishmaniasis. Evidence for expansion of distinct helper T cell subsets. J. Exp. Med. *169*, 59–72.

Iraji, F., and Sadeghinia, A. (2005). Efficacy of paromomycin ointment in the treatment of cutaneous leishmaniasis: results of a double-blind, randomized trial in Isfahan, Iran. Ann. Trop. Med. Parasitol. *99*, 3–9.

Isaac-Márquez, A.P., and Lezama-Dávila, C.M. (2003). Detection of pathogenic bacteria in skin lesions of patients with chiclero's ulcer. Reluctant response to antimonial treatment. Mem. Inst. Oswaldo Cruz *98*, 1093–1095.

Kamdar, K., Khakpour, S., Chen, J., Leone, V., Brulc, J., Mangatu, T., Antonopoulos, D.A., Chang, E.B., Kahn, S.A., Kirschner, B.S., et al. (2016). Genetic and metabolic signals during acute enteric bacterial infection alter the microbiota and drive progression to chronic inflammatory disease. Cell Host Microbe *19*, 21–31.

Kim, D.H., Chung, H.J., Bleys, J., and Ghohestani, R.F. (2009). Is paromomycin an effective and safe treatment against cutaneous leishmaniasis? A meta-analysis of 14 randomized controlled trials. PLoS Negl. Trop. Dis. *3*, e381.

Kobayashi, T., Glatz, M., Horiuchi, K., Kawasaki, H., Akiyama, H., Kaplan, D.H., Kong, H.H., Amagai, M., and Nagao, K. (2015). Dysbiosis and staphylococcus aureus colonization drives inflammation in atopic dermatitis. Immunity *42*, 756–766.

Kong, H.H., Oh, J., Deming, C., Conlan, S., Grice, E.A., Beatson, M.A., Nomicos, E., Polley, E.C., Komarow, H.D., Murray, P.R., et al.; NISC Comparative Sequence Program (2012). Temporal shifts in the skin microbiome associated with disease flares and treatment in children with atopic dermatitis. Genome Res. *22*, 850–859.

Kozich, J.J., Westcott, S.L., Baxter, N.T., Highlander, S.K., and Schloss, P.D. (2013). Development of a dual-index sequencing strategy and curation pipeline for analyzing amplicon sequence data on the MiSeq Illumina sequencing platform. Appl. Environ. Microbiol. *79*, 5112–5120.

Kristian, S.A., Datta, V., Weidenmaier, C., Kansal, R., Fedtke, I., Peschel, A., Gallo, R.L., and Nizet, V. (2005). D-alanylation of teichoic acids promotes group a streptococcus antimicrobial peptide resistance, neutrophil survival, and epithelial cell invasion. J. Bacteriol. *187*, 6719–6725.

Krolewiecki, A., Leon, S., Scott, P., and Abraham, D. (2002). Activity of azithromycin against Leishmania major in vitro and in vivo. Am. J. Trop. Med. Hyg. *67*, 273–277.

Kulkarni, M.M., McMaster, W.R., Kamysz, E., Kamysz, W., Engman, D.M., and McGwire, B.S. (2006). The major surface-metalloprotease of the parasitic protozoan, Leishmania, protects against antimicrobial peptide-induced apoptotic killing. Mol. Microbiol. *62*, 1484–1497.

Layegh, P., Ghazvini, K., Moghiman, T., Hadian, F., Zabolinejad, N., and Pezeshkpour, F. (2015). Bacterial contamination in cutaneous leishmaniasis: its effect on the lesions' healing course. Indian J. Dermatol. *60*, 211–212.

Loesche, M., Gardner, S.E., Kalan, L., Horwinski, J., Zheng, Q., Hodkinson, B.P., Tyldsley, A.S., Franciscus, C.L., Hillis, S.L., Mehta, S., et al. (2017). Temporal stability in chronic wound microbiota is associated with poor healing. J. Invest. Dermatol. *137*, 237–244.

Lopez Kostka, S., Dinges, S., Griewank, K., Iwakura, Y., Udey, M.C., and von Stebut, E. (2009). IL-17 promotes progression of cutaneous leishmaniasis in susceptible mice. J. Immunol. *182*, 3039–3046.

Lozupone, C.A., Li, M., Campbell, T.B., Flores, S.C., Linderman, D., Gebert, M.J., Knight, R., Fontenot, A.P., and Palmer, B.E. (2013). Alterations in the gut microbiota associated with HIV-1 infection. Cell Host Microbe *14*, 329–339.

Meisel, J.S., Hannigan, G.D., Tyldsley, A.S., SanMiguel, A.J., Hodkinson, B.P., Zheng, Q., and Grice, E.A. (2016). Skin microbiome surveys are strongly influenced by experimental design. J. Invest. Dermatol. *136*, 947–956.

Nagase, N., Sasaki, A., Yamashita, K., Shimizu, A., Wakita, Y., Kitai, S., and Kawano, J. (2002). Isolation and species distribution of staphylococci from animal and human skin. J. Vet. Med. Sci. *64*, 245–250.

Naik, S., Bouladoux, N., Wilhelm, C., Molloy, M.J., Salcedo, R., Kastenmuller, W., Deming, C., Quinones, M., Koo, L., Conlan, S., et al. (2012). Compartmentalized control of skin immunity by resident commensals. Science *337*, 1115–1119.

Naik, S., Bouladoux, N., Linehan, J.L., Han, S.J., Harrison, O.J., Wilhelm, C., Conlan, S., Himmelfarb, S., Byrd, A.L., Deming, C., et al. (2015). Commensal-dendritic-cell interaction specifies a unique protective skin immune signature. Nature *520*, 104–108.

Nakatsuji, T., Chen, T.H., Two, A.M., Chun, K.A., Narala, S., Geha, R.S., Hata, T.R., and Gallo, R.L. (2016). Staphylococcus aureus exploits epidermal barrier defects in atopic dermatitis to trigger cytokine expression. J. Invest. Dermatol. *136*, 2192–2200.

Natsuga, K., Cipolat, S., and Watt, F.M. (2016). Increased bacterial load and expression of antimicrobial peptides in skin of barrier-deficient mice with reduced cancer susceptibility. J. Invest. Dermatol. *136*, 99–106.

Neva, F.A., Ponce, C., Ponce, E., Kreutzer, R., Modabber, F., and Olliaro, P. (1997). Non-ulcerative cutaneous leishmaniasis in Honduras fails to respond to topical paromomycin. Trans. R. Soc. Trop. Med. Hyg. *91*, 473–475.

Nizet, V., Ohtake, T., Lauth, X., Trowbridge, J., Rudisill, J., Dorschner, R.A., Pestonjamasp, V., Piraino, J., Huttner, K., and Gallo, R.L. (2001). Innate antimicrobial peptide protects the skin from invasive bacterial infection. Nature *414*, 454–457.

Novais, F.O., Carvalho, L.P., Graff, J.W., Beiting, D.P., Ruthel, G., Roos, D.S., Betts, M.R., Goldschmidt, M.H., Wilson, M.E., de Oliveira, C.I., and Scott, P. (2013). Cytotoxic T cells mediate pathology and metastasis in cutaneous leishmaniasis. PLoS Pathog. *9*, e1003504.

Novais, F.O., Carvalho, L.P., Passos, S., Roos, D.S., Carvalho, E.M., Scott, P., and Beiting, D.P. (2015). Genomic profiling of human leishmania braziliensis lesions identifies transcriptional modules associated with cutaneous immunopathology. J. Invest. Dermatol. *135*, 94–101.

Oh, J., Freeman, A.F., Park, M., Sokolic, R., Candotti, F., Holland, S.M., Segre, J.A., and Kong, H.H.; NISC Comparative Sequencing Program (2013). The altered landscape of the human skin microbiome in patients with primary immunodeficiencies. Genome Res. *23*, 2103–2114.

Oliveira, M.R., Tafuri, W.L., Afonso, L.C., Oliveira, M.A., Nicoli, J.R., Vieira, E.C., Scott, P., Melo, M.N., and Vieira, L.Q. (2005). Germ-free mice produce high levels of interferon-gamma in response to infection with Leishmania major but fail to heal lesions. Parasitology *131*, 477–488.

Peschel, A., Otto, M., Jack, R.W., Kalbacher, H., Jung, G., and Götz, F. (1999). Inactivation of the dlt operon in Staphylococcus aureus confers sensitivity to defensins, protegrins, and other antimicrobial peptides. J. Biol. Chem. *274*, 8405–8410.

Peschel, A., Jack, R.W., Otto, M., Collins, L.V., Staubitz, P., Nicholson, G., Kalbacher, H., Nieuwenhuizen, W.F., Jung, G., Tarkowski, A., et al. (2001). Staphylococcus aureus resistance to human defensins and evasion of neutrophil killing via the novel virulence factor MprF is based on modification of membrane lipids with l-lysine. J. Exp. Med. *193*, 1067–1076.

Sadeghian, G., Ziaei, H., Bidabadi, L.S., and Baghbaderani, A.Z. (2011). Decreased effect of glucantime in cutaneous leishmaniasis complicated with secondary bacterial infection. Indian J. Dermatol. *56*, 37–39.

Salgado, V.R., Queiroz, A.T., Sanabani, S.S., Oliveira, C.I., Carvalho, E.M., Costa, J.M., Barral-Netto, M., and Barral, A. (2016). The microbiological signature of human cutaneous leishmaniasis lesions exhibits restricted bacterial diversity compared to healthy skin. Mem. Inst. Oswaldo Cruz *111*, 241–251.

Salzman, N.H., Hung, K., Haribhai, D., Chu, H., Karlsson-Sjöberg, J., Amir, E., Teggatz, P., Barman, M., Hayward, M., Eastwood, D., et al. (2010). Enteric defensins are essential regulators of intestinal microbial ecology. Nat. Immunol. *11*, 76–83.

Santos, Cda.S., Boaventura, V., Ribeiro Cardoso, C., Tavares, N., Lordelo, M.J., Noronha, A., Costa, J., Borges, V.M., de Oliveira, C.I., Van Weyenbergh, J., et al. (2013). CD8(+) granzyme B(+)-mediated tissue injury vs. CD4(+)IFNγ(+)-mediated parasite killing in human cutaneous leishmaniasis. J. Invest. Dermatol. *133*, 1533–1540.

Scharton-Kersten, T., Afonso, L.C., Wysocka, M., Trinchieri, G., and Scott, P. (1995). IL-12 is required for natural killer cell activation and subsequent T helper 1 cell development in experimental leishmaniasis. J. Immunol. *154*, 5320–5330.

Scott, P., and Novais, F.O. (2016). Cutaneous leishmaniasis: immune responses in protection and pathogenesis. Nat. Rev. Immunol. *16*, 581–592.

Song, S.J., Lauber, C., Costello, E.K., Lozupone, C.A., Humphrey, G., Berg-Lyons, D., Caporaso, J.G., Knights, D., Clemente, J.C., Nakielny, S., et al. (2013). Cohabiting family members share microbiota with one another and with their dogs. Elife *2*, e00458.

Späth, G.F., and Beverley, S.M. (2001). A lipophosphoglycan-independent method for isolation of infective Leishmania metacyclic promastigotes by density gradient centrifugation. Exp. Parasitol. *99*, 97–103.

Voronov, E., Dotan, S., Gayvoronsky, L., White, R.M., Cohen, I., Krelin, Y., Benchetrit, F., Elkabets, M., Huszar, M., El-On, J., and Apte, R.N. (2010). IL-1-induced inflammation promotes development of leishmaniasis in susceptible BALB/c mice. Int. Immunol. *22*, 245–257.

Wang, Q., Garrity, G.M., Tiedje, J.M., and Cole, J.R. (2007). Naive Bayesian classifier for rapid assignment of rRNA sequences into the new bacterial taxonomy. Appl. Environ. Microbiol. *73*, 5261–5267.

Zaph, C., Uzonna, J., Beverley, S.M., and Scott, P. (2004). Central memory T cells mediate long-term immunity to Leishmania major in the absence of persistent parasites. Nat. Med. *10*, 1104–1110.

Zenewicz, L.A., Yin, X., Wang, G., Elinav, E., Hao, L., Zhao, L., and Flavell, R.A. (2013). IL-22 deficiency alters colonic microbiota to be transmissible and colitogenic. J. Immunol. *190*, 5306–5312.

## STAR★METHODS

### KEY RESOURCES TABLE

| REAGENT or RESOURCE | SOURCE | IDENTIFIER |
|---|---|---|
| Antibodies | | |
| In vivo mAb Rat IgG2a Isotype Control | BioXcell | Cat# BE0089; RRID: AB_1107769 |
| In vivo mAb anti-IL-12 | BioXcell | Cat# BE0052; RRID: AB_1107700 |
| In vivo mAb anti-IL-17A | BioXcell | Cat# BE0173; RRID: AB_10950102 |
| In vivo mAb anti-IL-1R | BioXcell | Cat# BE0256; RRID: AB_2661843 |
| Brilliant Violet 650 anti-mouse CD4 | BioLegend | Cat# 100544; RRID: AB_11219790 |
| PerCp/Cy5.5 anti-mouse CD8b | BioLegend | Cat# 126610; RRID: AB_2260149 |
| PE-CF594 anti-Mouse γδ T Cell Receptor | BD Biosciences | Cat#563532; RRID: AB_2661844 |
| Alexa Fluor 700 anti-mouse CD45 | BioLegend | Cat# 103127; RRID: AB_493714 |
| eFluor 450 anti-mouse Ly6G | Thermo Fisher Scientific | Cat# 48-9668-80; RRID: AB_2637123 |
| Brilliant Violet 605 anti-mouse CD11b | BioLegend | Cat# 101239; RRID: AB_11125575 |
| APC anti-mouse IL-1 beta pro-form | Thermo Fisher Scientific | Cat# 17-7114-80; RRID: AB_10670739 |
| Alexa Fluor 488 anti-mouse IL-17A | Thermo Fisher Scientific | Cat# 53-7177-81; RRID: AB_763579 |
| PECy7 anti-mouse IFNγ | Thermo Fisher Scientific | Cat# 25-7311-41; RRID: AB_1257211 |
| Anti-mouse CD16/CD32 (Mouse block) | Thermo Fisher Scientific | Cat# 14-0161-86; RRID: AB_467135 |
| Bacterial and Virus Strains | | |
| *Staphylococcus xylosus* | This study | N/A |
| Alpha-hemolytic *Streptococcus* | This study | N/A |
| *Leishmania major* | WHO/MHOM/IL/80/Friedlin | N/A |
| Chemicals, Peptides, and Recombinant Proteins | | |
| 1-fluoro-2,4-dinitrobenzene (DNFB) | Sigma-Aldrich | Cat# D1529-10ML |
| Liberase TL | Roche | Cat# 05401054001 |
| DNase I | Sigma-Aldrich | Cat# 4536282001 |
| Brefeldin A | Sigma-Aldrich | Cat# B7651-25MG |
| Ionomycin | Sigma-Aldrich | Cat# I3909-1ML |
| Critical Commercial Assays | | |
| LIVE/DEAD Fixable Aqua Dead Cell Stain Kit | Molecular Probes | Cat# L34957 |
| RNeasy Mini Kit | QIAGEN | Cat# 74106 |
| High capacity RNA to cDNA Kit | Applied Biosystems | Cat# 4387406 |
| SYBR Green PCR Master Mix | Applied Biosystems | Cat# 4309155 |
| PureLink Genomic DNA Mini Kit | Invitrogen | Cat# K182002 |
| MasterPure Yeast DNA Purification Kit | Epicenter | Cat# MPY80200 |
| PowerSoil DNA Isolation Kit | MoBio | Cat# 12888-100 |
| Deposited Data | | |
| 16S rRNA gene sequence data | This study | SRA: RJNA389688 |
| Experimental Models: Organisms/Strains | | |
| Mouse: C57BL/6 | Charles River Laboratories | Strain code# 556 |
| Mouse: BALB/c | Charles River Laboratories | Strain code# 555 |
| Oligonucleotides | | |
| See Table S3 | This study | N/A |
| Software and Algorithms | | |
| FlowJo | N/A | http://docs.flowjo.com/vx/ |
| QIIME 1.8.0 | Caporaso et al., 2010 | http://qiime.org/ |
| R Statistical Software | N/A | https://www.r-project.org/ |
| Prism (GraphPad Software) | N/A | https://www.graphpad.com/scientific-software/prism/ |

## CONTACT FOR REAGENT AND RESOURCE SHARING

Further information and requests for resources and reagents should be directed to and will be fulfilled by the Lead Contact, Elizabeth Grice (egrice@upenn.edu).

## EXPERIMENTAL MODEL AND SUBJECT DETAILS

### Mice

Female C57BL/6 and BALB/c mice 6-8 weeks old were purchased from the Charles River Laboratories (Durham, NC). All mice were maintained in specific pathogen-free facilities at the University of Pennsylvania. The mice were under the care of a veterinarian and were healthy, immunocompetent, and required no drugs or treatment prior to experimentation. Cages were changed twice per week with glove changes between handling each cage. Unless stated otherwise, a minimum of 5 mice were used based on variability observed in previous experiments with *L. major*. Mice were randomly assigned to experimental groups by investigators. Investigators were not blinded in this study. Prior to infection, mice were anesthetized using a ketamine and xylazine mixture and monitored until the mice were fully awake. At the end of the experiments, mice were humanely euthanized using carbon dioxide inhalation. All procedures involving mice were performed in accordance with the guidelines of the University of Pennsylvania Institutional Animal Care and Use Committee (IACUC).

### Human Cutaneous Leishmaniasis Subjects

All cutaneous leishmaniasis patients were seen at the health post in Corte de Pedra, Bahia, Brazil, which is a well-known area of *L. braziliensis* transmission. The criteria for diagnosis were a clinical picture characteristic of cutaneous leishmaniasis in conjunction with documentation of DNA of *L. braziliensis* by PCR, or parasite isolation or documentation of amastigotes in lesion biopsies by histopathology. In all cases, swabs were collected before therapy. There were 44 patients, both male (72.7%) and female (27.3%), with a median age of 27 years. This study was conducted according to the principles specified in the Declaration of Helsinki and under local ethical guidelines (Ethical Committee of the Maternidade Climerio de Oliveira, Salvador, Bahia, Brazil; and the University of Pennsylvania Institutional Review Board). This study was approved by the Ethical Committee of the Federal University of Bahia (Salvador, Bahia, Brazil) (010/10) and the University of Pennsylvania IRB (Philadelphia, PA) (813390). All patients provided written informed consent for the collection of samples and subsequent analysis.

### Parasite and Bacterial Cultures

*L. major* (WHO/MHOM/IL/80/Friedlin wild-type *L. major*) promastigotes were grown to the stationary phase in Schneider's *Drosophila* medium (GIBCO BRL, Grand Island, NY, USA) supplemented with 20% heat-inactivated fetal bovine serum (FBS, Invitrogen USA), 2 mM L-glutamine, 100 U of penicillin and 100 μg of streptomycin per mL. Infective-stage promastigotes (metacyclics) were isolated from 4-5 day old (*L. major*) stationary culture by density gradient separation by Ficoll (Sigma) (Späth and Beverley, 2001). An isolate of *S. xylosus* and alpha-hemolytic *Streptococcus* was cultured from the ears of *L. major* infected mice. For topical associations and infections, the bacteria was cultured in Brain heart infusion (BHI) media (Remel, Lenexa, KS, USA) shaking for 12 hr at 37°C.

## METHOD DETAILS

### Leishmania Infection and In Vivo Antibody Depletions

Mice were inoculated intradermally in the ear with 10 μL of PBS containing $2 \times 10^6$ *L. major* metacyclic promastigotes. Lesion development was measured weekly by ear thickness with a digital caliper (Fisher Scientific). Mice were also assessed for pathology, using the following score system: no lesion (0), swelling/redness (1), deformation of the ear pinna (2), ulceration (3), partial tissue loss (4), and total tissue loss (5). Parasite burden in lesion tissues was assessed using a limiting dilution assay as previously described (Zaph et al., 2004). In specified experiments, mice were treated with 500 μg of anti-IL-12 mAb (BioXcell, clone R1-5D9, RRID: AB_1107700) one day prior to infection and then twice per week for the duration of the experiment. Equal amounts of an isotype control, Rat IgG2a (BioXcell, clone 2A3, RRID: AB_1107769) was given in all experiments using in vivo antibody treatments.

### Bacterial Topical Associations, Intradermal Infections, and CFU Quantification

For topical associations, $10^8$-$10^9$ CFUs of bacteria were applied to the entire mouse body using sterile cotton swabs, every other day for a total of 4 times. For intradermal infections, mice were inoculated with 10 μL of $10^8$-$10^9$ CFU bacteria/mL culture. For CFU quantification, the dermal sheets of the mouse ears were homogenized in 1mL of PBS using a tissue homogenizer (FastPrep-24, MP Biomedical) and plated on tryptic soy blood agar (Remel) or mannitol salt agar (Acumedia) in serial dilutions. Plates were incubated overnight at 37°C and CFUs were counted the next day.

### Contact Hypersensitivity and Antibody Treatments

For sensitization, 1-fluoro-2,4-dinitrobenzene (DNFB) (Sigma-Aldrich) was added to a 3:1 acetone:olive oil dissolvent to get a final concentration of 0.5%. Mice were treated on the belly with 30 μL of the mixture. During the challenge phase, mice were treated with 20 μL of 0.3% DNFB (in 3:1 acetone:olive oil) on the ear once a day, for a total of 3 days. The mice were euthanized 24 hr after

the last challenge. In some experiments, mice were treated with 500 μg of a Rat IgG2a isotype monoclonal antibody (BioXcell, clone 2A3, RRID: AB_1107769), an anti-mouse IL-17A monoclonal antibody (BioXcell, clone 17F3, RRID: AB_10950102), or an anti-mouse IL-1R monoclonal antibody (BioXcell, clone JAMA-147, RRID: AB_2661843), one day prior and one day after the first challenge with DNFB.

### Preparation of Dermal Sheets

The dorsal and ventral sides of the mouse ear were split mechanically and placed dermis side down in a 24 wells plate in RPMI 1640 containing 0.25 mg/mL of Liberase TL (Roche, Diagnostics Corp.) and 10 μg/mL DNase I (Sigma-Aldrich). Ears were incubated for 90 min at 37°C in a 24-well plate. Dermal cell suspensions were prepared by dissociation on 40 μm cell strainer (Falcon) in PBS containing 0.05% BSA and 20 μM EDTA.

### Antibodies and Flow Cytometry

Single cell suspensions from the ear were obtained as described above. For analysis of surface markers and intracellular cytokines, some cells were incubated for 4 hr with 10 μg/mL of brefeldin A, 50 ng/mL of PMA and 500 ng/mL ionomycin (Sigma-Aldrich). Before staining, cells were incubated with anti-mouse CD16/CD32 mouse Fc block (Thermo Fisher Scientific, RRID: AB_467135) and 10% rat-IgG in PBS containing 0.1% BSA. Cells were stained for dead cells with LIVE/DEAD Fixable Aqua Dead Cell Stain Kit (Molecular Probes) and surface markers (CD4 [BioLegend, clone RM4-5, RRID: AB_11219790], CD8β [BioLegend, clone YTS156.7.7, RRID: AB_2260149], TCRγδ [BD Biosciences, clone GL3, RRID: AB_2661844], CD45 [Thermo Fisher Scientific, clone 30-F11, RRID: AB_493714], Ly6G [Thermo Fisher Scientific, clone 1A8-Ly6g, RRID: AB_2637123], CD11b [BioLegend, clone M1/70, RRID: AB_11125575]) followed by fixation with 2% of formaldehyde and permeablization with 0.2% saponin/PBS. Intracellular cytokine staining was performed for pro-IL-1β (Thermo Fisher Science, clone NJTEN3, RRID: AB_10670739), IL-17 (Thermo Fisher Scientific, clone eBio17B7, RRID: AB_763579), and IFN-γ (Thermo Fisher Scientific, clone XMG1.2, RRID: AB_1257211). The data were collected using LSRII flow cytometer (BD) and analyzed using FlowJo software (Tree Star).

### RNA Isolation, Purification, and Quantitative Real-Time PCR

Total RNA was extracted from ear tissue samples in 500 μL of RLT lysis buffer (QIAGEN). The sample was homogenized using a tissue homogenizer (FastPrep-24, MP Biomedical), and total RNA was extracted according to the recommendations of the manufacturer and further purified using the RNeasy Mini kit (QIAGEN). RNA was reverse transcribed using high capacity RNA-to-cDNA Kit (Applied Biosystems). Real-time RT-PCR was performed on a ViiA 7 Real-Time PCR System (Applied Biosystems). Relative quantities of mRNA for several genes were determined using SYBR Green PCR Master Mix (Applied Biosystems) and by the comparative threshold cycle method, as described by the manufacturer. mRNA levels for each sample were normalized to the ribosomal protein S11 gene (RPS11). The primer sequences are reported in Table S3.

### Microbiota Collection, Sequencing, and Analysis

Microbiota samples were collected from the ear of mice using a swab (Catch-all Sample Collection Swab, Epicenter) moistened in Yeast Cell Lysis Buffer (from MasterPure Yeast DNA Purification Kit; Epicenter). DNA was isolated from swab specimens using the PureLink Genomic DNA Mini Kit (Invitrogen) and amplification of the 16S-V4 region for the murine samples, and 16S-V1-V3 region for the human samples, was performed as previously described (Hannigan et al., 2014; Meisel et al., 2016). Sequencing of 16S rRNA amplicons was performed at the Penn Next Generation Sequencing Core using the Illumina MiSeq platform with 150 bp paired-end 'V4' chemistry for murine samples and with 300 bp paired-end 'V1-V3′ chemistry for the human samples. For the fecal samples, DNA was isolated using the PowerSoil DNA Isolation Kit (Mo Bio) and sequencing of the 16S rRNA amplicons was conducted using 250bp paired-end 'V4' chemistry with dual index primers (Kozich et al., 2013).

## QUANTIFICATION AND STATISTICAL ANALYSIS

### Pre-processing and Community Characterization of 16S rRNA Sequence Data

Sequence pre-processing followed methods previously described (Hannigan et al., 2014), but modified by subsampling at 5000 sequences per sample for murine samples, and at 1000 sequences per sample for human samples. QIIME 1.8.0 (Caporaso et al., 2010) was used for initial stages of sequence analysis. Sequences were clustered into OTUs (operational taxonomic units, a proxy for 'species') using UCLUST (Edgar, 2010) at 97% sequence similarity. Bacterial diversity was calculated using the following alpha diversity indices: Shannon diversity index and the number of observed OTUs. Relative abundance of bacteria was calculated based on taxonomic classification of sequences using the RDP classifier (Wang et al., 2007) at a confidence threshold of 0.8. Microbiota data was analyzed with the R statistical software environment (https://www.r-project.org/). Statistical significance was determined using two-sample Wilcoxon tests and corrected for multiple comparisons by FDR where appropriate. Dirichlet multinomial mixture modeling was performed using the R package Dirichlet Multinomial and calculated as previously reported (Loesche et al., 2017).

### Sample Sizes

n represents the number of patients, mice, or swabs collected from each mouse as described in legends of each figure.

### Statistical Analysis

Results represent means ± SEM. Data were analyzed using Prism 7.0 (GraphPad Software, San Diego, CA). Statistical significance was determined by one-way ANOVA when comparing more than two groups and by an unpaired two-tailed Student's t test to compare means of lesion sizes, parasite burdens, and cytokine production from different groups of mice. Variances were equal between experimental groups. Statistically significant differences were defined as * when p values were $< 0.05$, ** $p < 0.01$, *** $p < 0.001$, and **** $p < 0.0001$.

## DATA AND SOFTWARE AVAILABILITY

The accession number for the 16S rRNA gene sequence data reported in this paper is SRA: PRJNA389688.

**Cell Host & Microbe, Volume *22***

## Supplemental Information

# Cutaneous Leishmaniasis Induces a Transmissible Dysbiotic Skin Microbiota that Promotes Skin Inflammation

**Ciara Gimblet, Jacquelyn S. Meisel, Michael A. Loesche, Stephen D. Cole, Joseph Horwinski, Fernanda O. Novais, Ana M. Misic, Charles W. Bradley, Daniel P. Beiting, Shelley C. Rankin, Lucas P. Carvalho, Edgar M. Carvalho, Phillip Scott, and Elizabeth A. Grice**

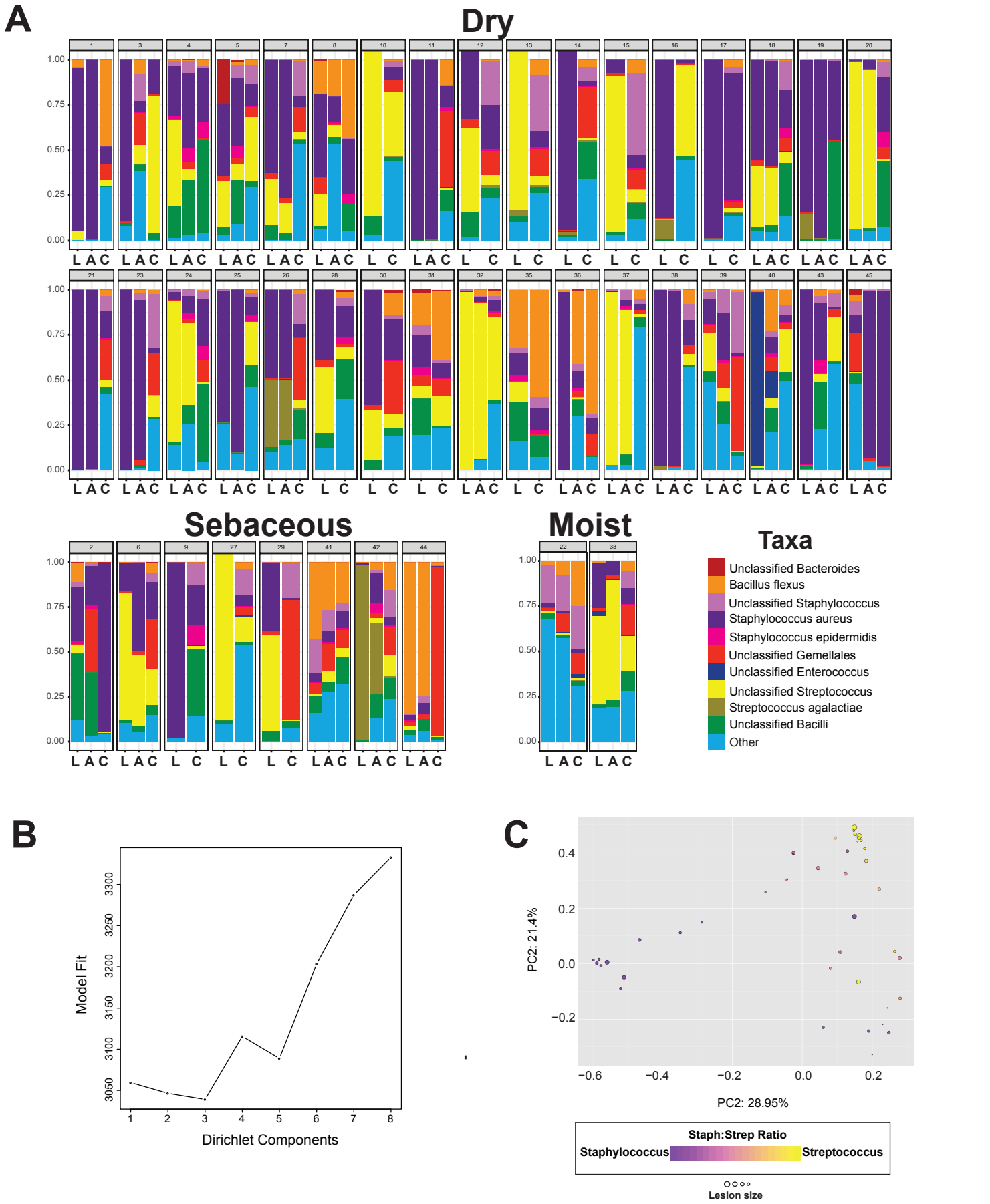


**Supplemental Figure 1. Samples from patients are diverse and lesions cluster into 3 community types, Related to Figure 1.** (A) Stacked bar charts represent the proportion of the top 10 taxa present in each sample. Patients are identified by number and skin type is identified as lesion (L), adjacent skin sites (A), or contralateral skin sites (C). (B) Laplace approximation of model evidence was used to measure the model fit. The lowest value (3) indicates the best fit for the model. (C) PCoA values for weighted UniFrac analysis were plotted and colored based on the ratio of the abundances of Staphylococcus spp. to Streptococcus spp. in each lesions sample and circle size is based on size of the lesion of each sample.

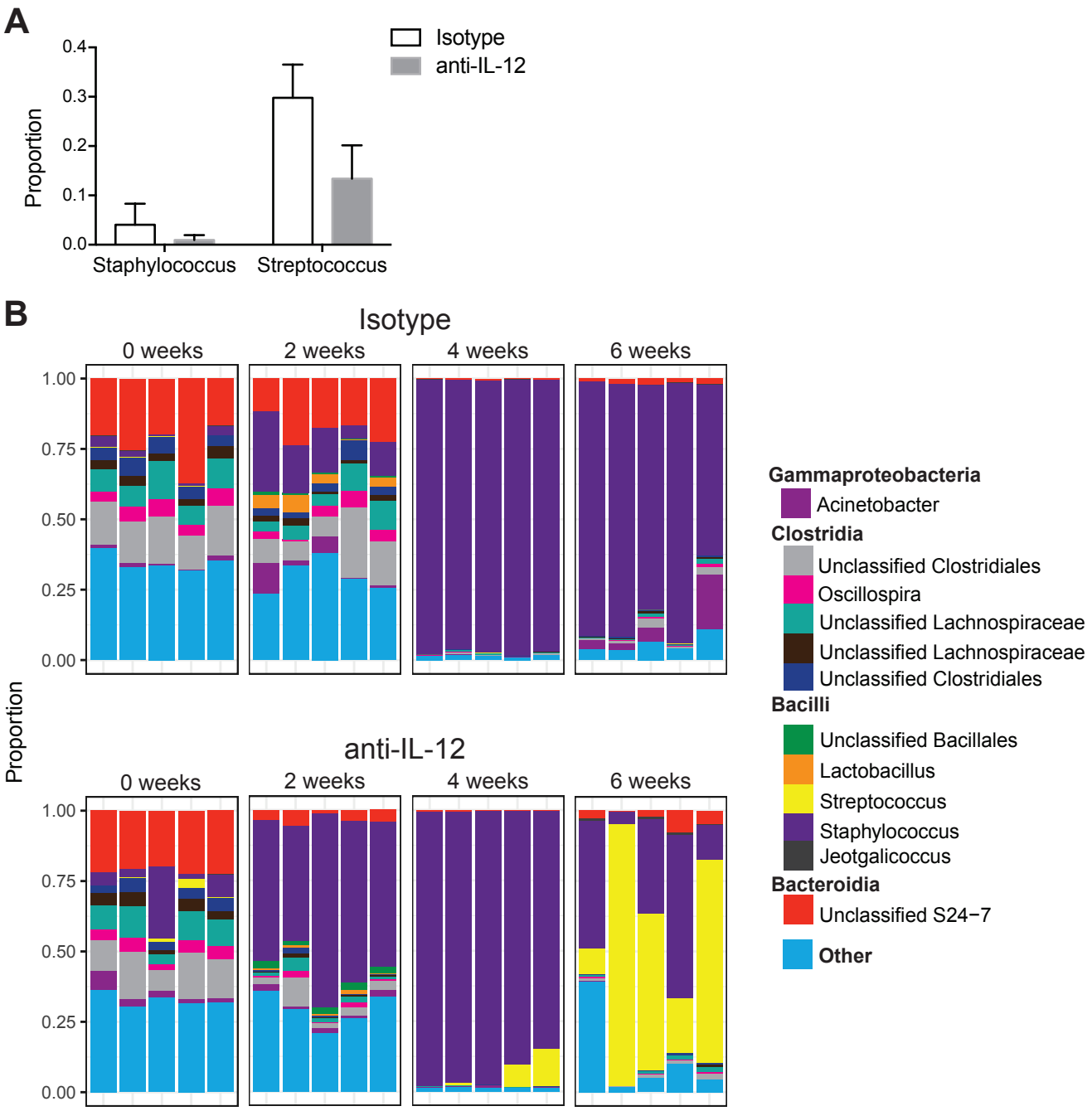


**Supplemental Figure 2. Anti-IL-12 treatment alters the skin microbiota during *L. major* infection, but not on naive skin, Related to Figure 3.** (A) C57BL/6 mice were treated with an isotype or anti-IL-12 mAB twice a week. Swabs were collected prior to treatment and at 2 weeks post-treatment to assess the proportion of Staphylococcus spp. and Streptococcus spp. by 16S rRNA gene analysis. Data are representative of one independent experiment (n = 1 swab of each ear from 3 mice in each group). (B) Isotype and anti-Il-12 mAB treated mice were intradermally infected in the ear with *L. major* parasites. Swabs were collected for 16S rRNA gene sequencing at 0 weeks (before treatment and infection) and at 2, 4, and 6 weeks post-infection. Stacked bar charts represent the proportion of each taxa present within the samples. Data are representative of two independent experiments (n = 1 lesional swab from 10 mice in each group).

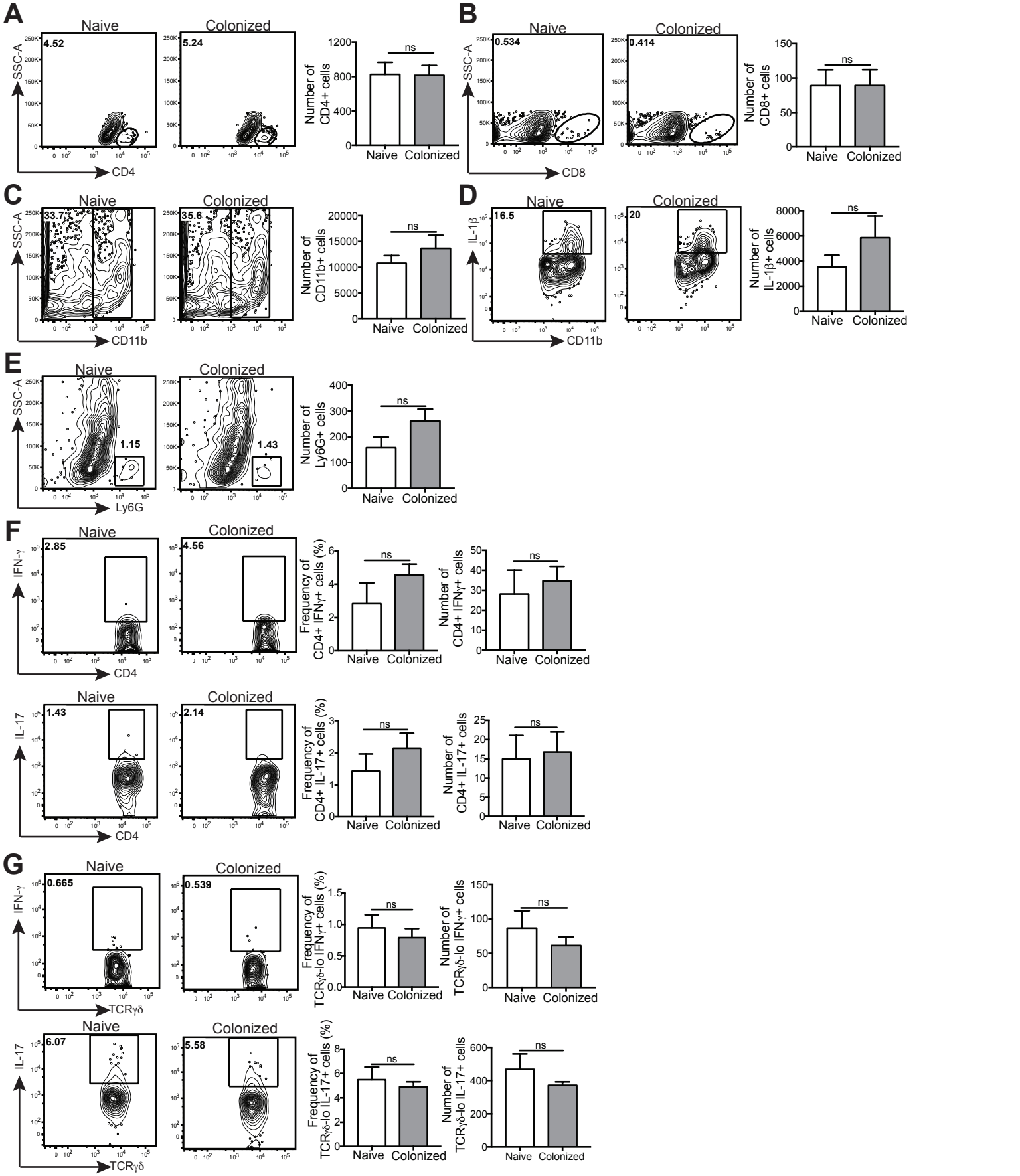


**Supplemental Figure 3. Dysbiosis due to *S. xylosus* colonization does not alter the immune response or cytokine production in naive skin, Related to Figure 4.** C57BL/6 mice were topically colonized with $10^8$-$10^9$ *S. xylosus* every other day for a total of 4 applications; naïve mice were unassociated. Flow cytometry analysis was performed for the frequency and total cell number of (A) CD4+ T cells (B) CD8+ T cells (C) CD11b+ cells (D) CD11b+ IL-1β+ cells (E) Ly6G+ cells (F) CD4+ IFNγ+ and CD4+ IL-17+ and (G) TCRγδ+ IFNγ+ and TCRγδ+ IL-17+ cells in the ears of naïve or colonized mice 14 days post-association. Cells were pregated on live, singlet, CD45+ cells. Flow cytometry plots are representatives of each group. Data are representative of two independent experiments (n = 1 ear tissue from 4 mice in each group). ns = not significant.

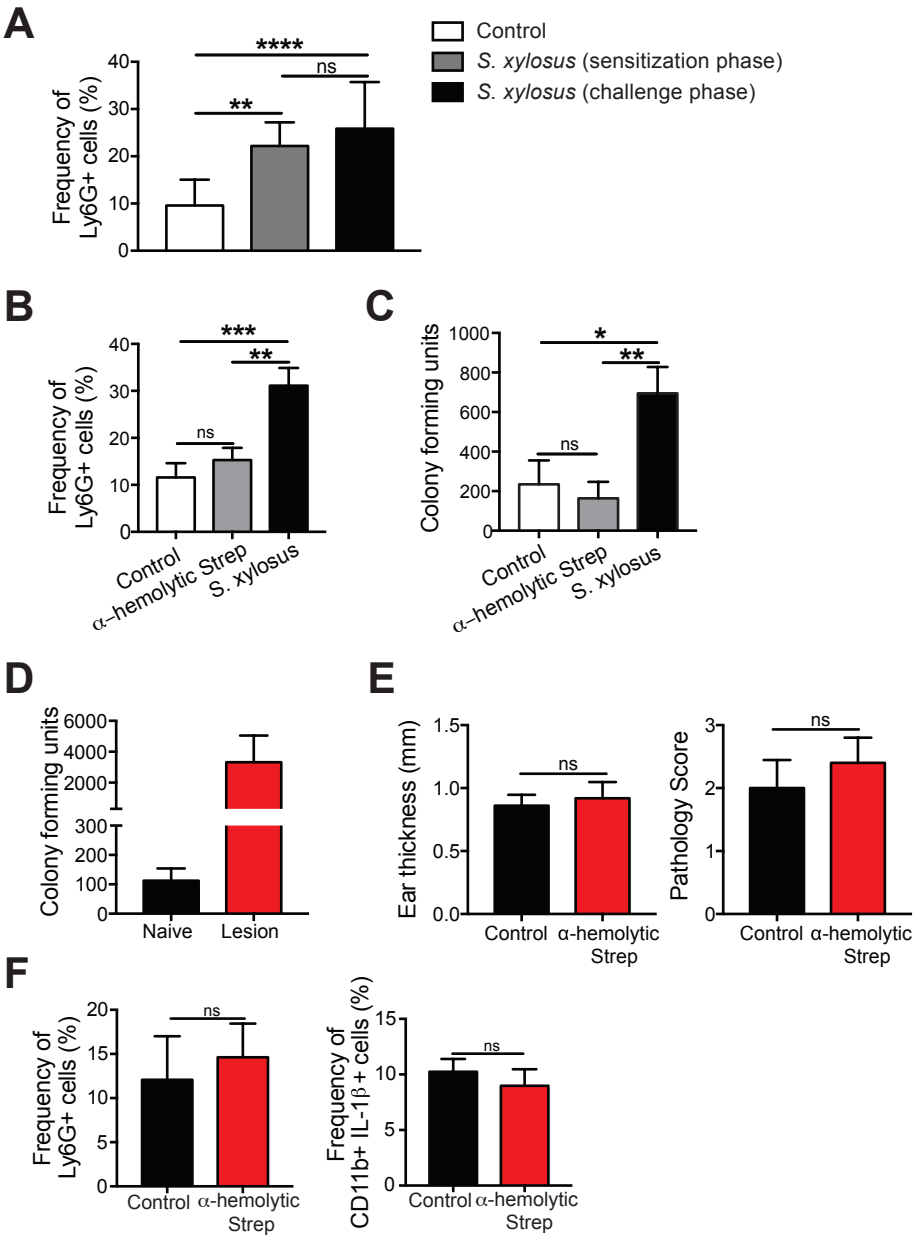


**Supplemental Figure 4. *S. xylosus* only exacerbates inflammation during a barrier breach, while *Streptococcus* does not, Related to Figure 5.** (A) C57BL/6 mice were topically colonized with $10^8$-$10^9$ CFU of *S. xylosus* prior to the sensitization phase or on each day of the challenge phase of DNFB treatment. Control mice were unassociated, then sensitized and challenged with DNFB. Bar graphs of skin cells depict the frequency of Ly6G+ cells present in the ear skin on day 8. Data are representative of one experiment (n = 1 ear tissue from 5 mice in each group). (B) C57BL/6 mice were topically associated with $10^8$-$10^9$ CFU of an alpha hemolytic *Streptococcus* isolate or *S. xylosus* every other day for 4 applications and control C57BL/6 mice were left unassociated. The next day, all mice were treated on the belly with DNFB. Five days later, mice were challenged with DNFB. Bar graphs depict the frequency of Ly6G+ cells present in the ear skin. (C) Colony forming units were measured after skin homogenates were cultured on tryptic soy blood agar plates overnight from the ears of control and alpha hemolytic *Streptococcus* or *S. xylosus* associated mice. Data are representative of two independent experiments (n = 1 ear tissue from 5 mice in each group). (D) C57BL/6 mice were intradermally infected with *L. major*. At 3 weeks post-infection, mice were topically associated with $10^8$-$10^9$ CFU of an alpha hemolytic *Streptococcus* isolate every other day for 4 applications and control C57BL/6 mice were left unassociated. Colony forming units were measured after skin homogenates were cultured on tryptic soy blood agar plates overnight from the ear skin of control and alpha hemolytic *Streptococcus* associated mice. (E) Lesion size and pathology were assessed after colonization. (F) Bar graphs of skin cells depict the frequency of Ly6G+ and IL-1β+ cells present in the ear skin. Data are representative of one experiment (For colonized naive mice, n = 1 ear tissue from 3 mice; for colonized infected mice, n = 1 ear tissue from 5 mice; for uncolonized control mice, n = 1 ear tissue from 5 mice). ns = not significant; *, $p < 0.05$; **, $p < 0.01$; ***, $p < 0.001$; ****, $p < 0.0001$.

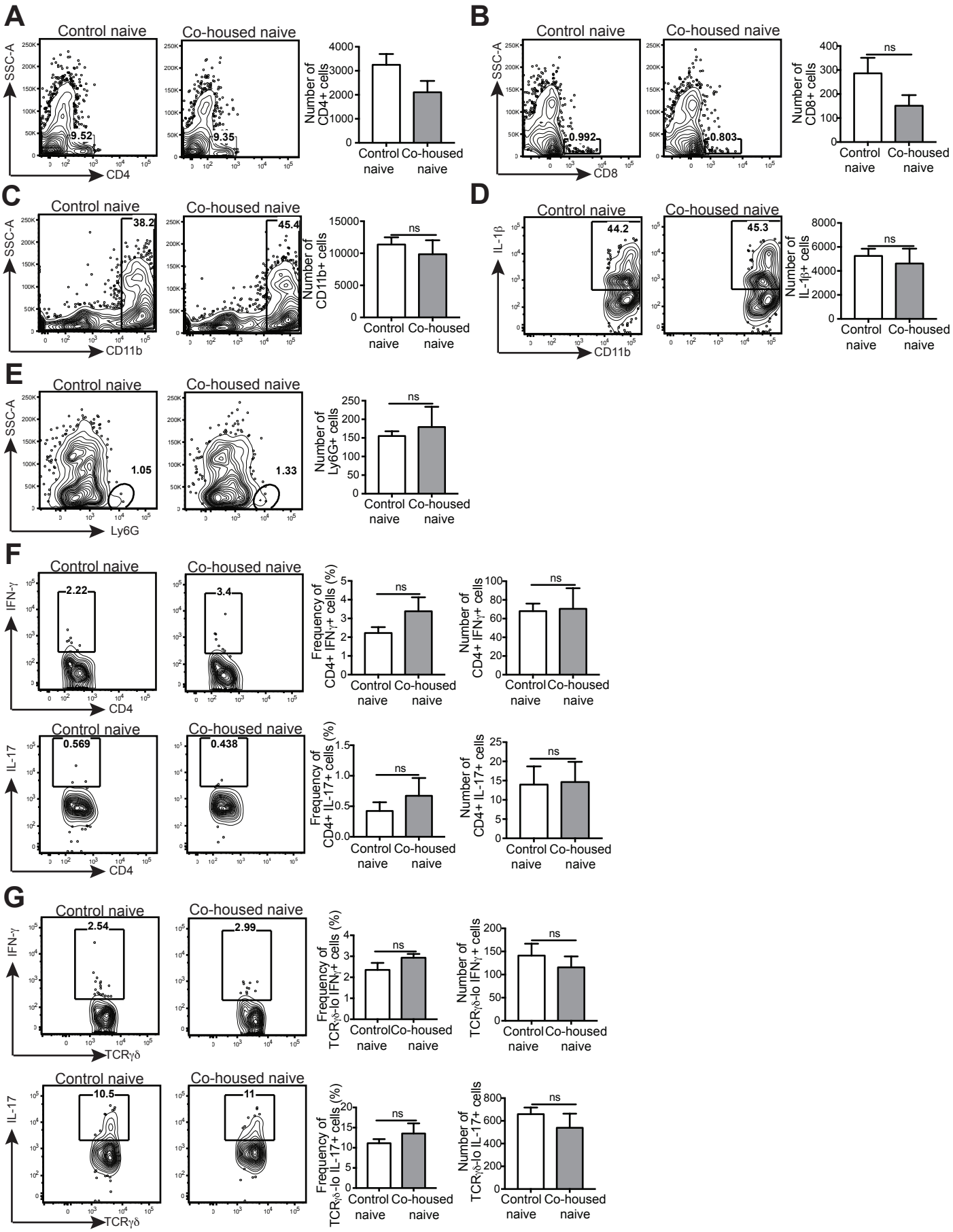


**Supplemental Figure 5. Dysbiosis due to co-housing does not alter the immune response or cytokine production in naive skin, Related to Figure 6.** Naïve C57BL/6 mice were co-housed with L. major infected mice for 6 weeks, while control naïve mice were housed separately. Cells were isolated from the ears of co-housed naïve mice and control naïve mice. Flow cytometry analysis was performed for the frequency and total cell number of (A) CD4+ T cells (B) CD8+ T cells (C) CD11b+ cells (D) CD11b+ IL-1β+ cells (E) Ly6G+ cells (F) CD4+ IFNγ+ and CD4+ IL-17+ and (G) TCRγδ+ IFNγ+ and TCRγδ+ IL-17+ cells in the ears of naïve or co-housed mice. Cells were pregated on live, singlet, CD45+ cells. Flow cytometry plots are representatives of each group. Data are representative of one experiment (Co-housed naïve, n = 1 ear tissue from 4 mice; control naïve, n = 1 ear tissue from 5 mice). ns = not significant.

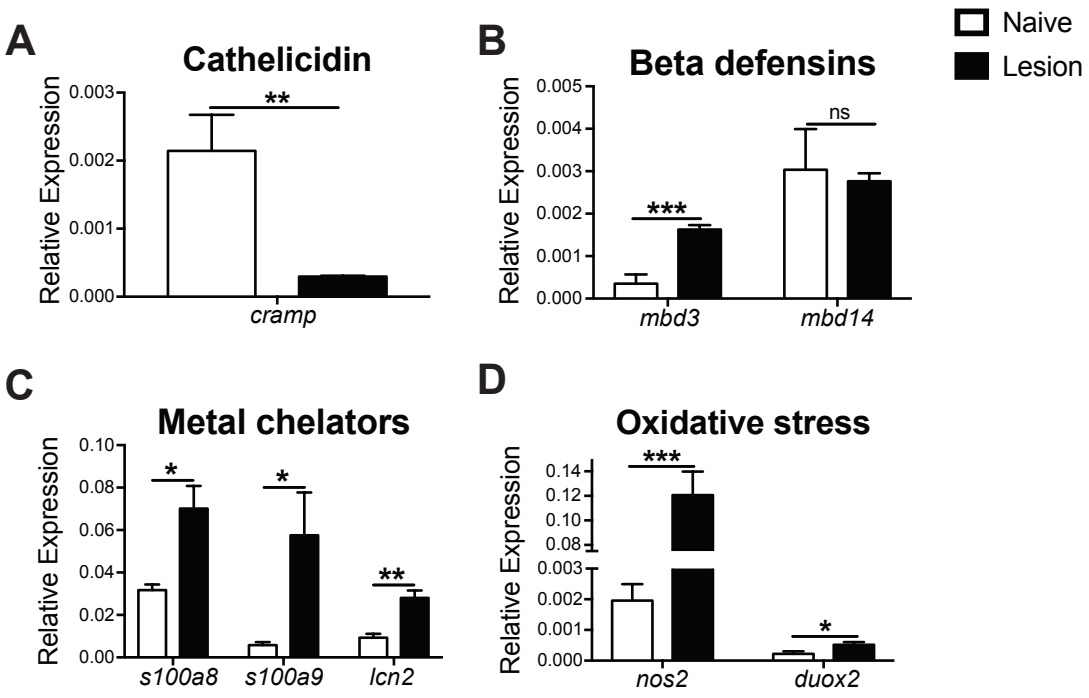


**Supplemental Figure 6. *L. major* infection alters the expression of antimicrobial peptides in the skin, Related to Figure 1.** C57BL/6 mice were intradermally infected with *L. major* in the ear for 5 weeks. Ear skin was harvested from naive and infected mice and mRNA expression was assessed for (A) the murine cathelicidin gene, (B) beta defensin genes, (C) metal chelators genes and (D) oxidative stress genes. Data are representative of two independent experiments (For naive group, n = 1 ear tissue from 4 mice; for infected mice n = 1 ear tissue from 7 mice). ns = not significant; *, $p < 0.05$; **, $p < 0.01$; ***, $p < 0.001$.

| Subject ID | Sex | Age | Body Site | Lesion Size (mm2) | Duration of Lesion (Days) | Skin Test (mm2) |
|---|---|---|---|---|---|---|
| 1 | Male | 22 | Leg | 396 | 30 | 440 |
| 2 | Male | 43 | Neck | 216 | 30 | 225 |
| 3 | Male | 18 | Ankle | NA | 40 | 300 |
| 4 | Male | 24 | Leg | 225 | 40 | 144 |
| 5 | Male | 20 | Leg | 660 | 90 | 725 |
| 6 | Male | 16 | Back | 500 | 30 | 440 |
| 7 | Female | 30 | Leg | 544 | 21 | 225 |
| 8 | Male | 36 | Thigh | 437 | 30 | Negative |
| 9 | Male | 31 | Face | 840 | 60 | 300 |
| 10 | Male | 22 | Arm | 49 | 30 | 400 |
| 11 | Female | 24 | Thigh | 25 | 30 | 210 |
| 12 | Female | 39 | Leg | 70 | 30 | 130 |
| 13 | Male | 22 | Leg | 3300 | 40 | 110 |
| 14 | Female | 45 | Leg | 180 | 30 | 378 |
| 15 | Male | 26 | Leg | 90 | 10 | 260 |
| 16 | Male | 21 | Arm | 200 | 60 | 400 |
| 17 | Female | 33 | Leg | 380 | 40 | NA |
| 18 | Male | 21 | Leg | 780 | 21 | 228 |
| 19 | Female | 20 | Leg | 80 | 30 | 100 |
| 20 | Male | 29 | Leg | 500 | 60 | 180 |
| 21 | Female | 35 | Leg | 100 | 60 | 255 |
| 22 | Male | 37 | Foot | 24 | 60 | 300 |
| 23 | Female | 26 | Arm | 130 | 30 | 285 |
| 24 | Male | 25 | Leg | 150 | 21 | 180 |
| 25 | Male | 50 | Leg | 270 | 30 | 272 |
| 26 | Male | 55 | NA | 1575 | 60 | 1085 |
| 27 | Male | 18 | Head | 192 | 34 | 130 |
| 28 | Male | 19 | Leg | 480 | 14 | 208 |
| 29 | Female | 24 | Abdomen | 325 | NA | 700 |
| 30 | Male | 40 | Leg | 130 | 20 | 460 |
| 31 | Male | 57 | Leg | 35 | 45 | 132 |
| 32 | Male | 18 | Leg | 49 | 20 | 400 |
| 33 | Male | 19 | Foot | 306 | 15 | 441 |
| 34 | Male | 28 | Leg | 25 | 15 | 49 |
| 35 | Male | 39 | Leg | 77 | 30 | 255 |
| 36 | Male | 31 | Leg | 330 | 90 | 130 |
| 37 | Female | 24 | Leg | 1476 | 60 | 625 |
| 38 | Male | 63 | Leg | 272 | 20 | 196 |
| 39 | Male | 20 | Arm | 1377 | 45 | 225 |
| 40 | Female | 16 | Chest | 30 | 20 | 156 |
| 41 | Female | 24 | Back | 255 | 30 | 144 |
| 42 | Female | 64 | Leg | 216 | 30 | NA |
| 43 | Male | 33 | Abdomen | 207 | 40 | 289 |
| 44 | Male | 59 | Thigh | 340 | 90 | 255 |

**Supplemental Table 1. Information about samples collected from cutaneous leishmaniasis patients, Related to Figure 1.** Swabs were collected from these cutaneous leishmaniasis patients prior to treatment. All cutaneous leishmaniasis patients were seen at the health post in Corte de Pedra, Bahia, Brazil, which is a well-known area of L. braziliensis transmission. The criteria for diagnosis were a clinical picture characteristic of cutaneous leishmaniasis in conjunction with parasite isolation or a positive delayed-type hypersensitivity response to Leishmania antigen, plus histological features of cutaneous leishmaniasis.

| Taxa | Cluster 1 | Cluster 2 | Cluster 3 |
|---|---|---|---|
| Staphylococcus aureus | 0.788992731 | 0.16077901 | 0.049802691 |
| Unclassified Streptococcus 1 | 0.022511662 | 0.11087683 | 0.814618671 |
| Unclassified Bacilli | 0.04901982 | 0.10691883 | 0.018451401 |
| Unclassified Gemellales | 0.030965307 | 0.06667456 | 0.013448359 |
| Unclassified Staphylococcus 1 | 0.013819064 | 0.06478127 | 0.005975455 |
| Bacillus flexus | 0.002613152 | 0.06594624 | 0.00479366 |
| Unclassified Staphylococcus 2 | 0.010710605 | 0.02253503 | 0.004936899 |
| Unclassified Streptococcus 2 | 0.007199348 | 0.0130796 | 0.01322084 |
| Unclassified Bacillales | 0.002463076 | 0.02473744 | 0.001617316 |
| Staphylococcus epidermidis | 0.001303855 | 0.02767135 | 0.001574108 |

**Supplemental Table 2. DMN Clusters top 10 discriminating taxa, Related to Figure 1.**
Bacteria represent the top 10 discriminating taxa present in each DMN cluster. Numbers depict the proportion of each taxa in clusters 1-3.

| Primer | Sequence |
|---|---|
| *Rps11*, forward | 5’-CGTGACGAAGATGAAGATGC-3’ |
| *Rps11,* reverse | 5’-GCACATTGAATCGCACAGTC-3 |
| *Il17*, forward | 5'-CATGAGTCCAGGGAGAGCTT-3' |
| *Il17,* reverse | 5'-GCTGAGCTTTGAGGGATGAT-3' |
| *Tnfa*, forward | 5'-TCACTGGAGCCTCGAATGTC-3' |
| *Tnfa*, reverse | 5'-GTGAGGAAGGCTGTGCATTG-3' |
| *Il1b*, forward | 5'-TTGACGGACCCCAAAAGAT-3’ |
| *Il1b*, reverse | 5’- GATGTGCTGCTGCGAGATT-3’ |
| *Cxcl1*, forward | 5'-GCACCCAAACCGAAGTCATA-3' |
| *Cxcl1*, reverse | 5'-CTTGGGGACACCTTTTAGCA-3' |
| *Ccl2*, forward | 5’-GCTTCTGGGCCTGCTGTTCA-3 |
| *Ccl2*, reverse | 5’-AGCTCTCCAGCCTACTCATT-3’ |

**Supplemental Table 3. Oligonucleotide sequences, Related to Figure 4.**
Primers used for RT-PCR on whole ear skin tissue.